Physical and biochemical averaged vertical profiles in the Mediterranean regions: an important tool to trace the climatology of water masses and to validate incoming data from operational oceanography

B. Manca[a,*], M. Burca[b], A. Giorgetti[a], C. Coatanoan[c], M.-J. Garcia[d], A. Iona[e]

[a] *Istituto Nazionale di Oceanografia e di Geofisica Sperimentale-OGS, Borgo Grotta Gigante 42c, 34010 Sgonico, Trieste, Italy*
[b] *National Institute for Marine Research and Development "Grigore Antipa", Constanta, Romania*
[c] *IFREMER/SISMER, BP 70, 29280 Plouzane, France*
[d] *Instituto Espanol de Oceanografia-IEO, c. Corazon de Maria 8, 28002 Madrid, Spain*
[e] *National Centre for Marine Research, NCMR, Aghios Kosmas-Hellinikon, 16604 Athens, Greece*

Abstract

Seasonally and spatially averaged vertical profiles of temperature, salinity, dissolved oxygen, nutrients and chlorophyll-*a* have been computed from in situ observations in different regions of the Mediterranean Sea using the recently released EU/ MEDAR/MEDATLAS II and EU/MTPII/MATER databases. The regions have been defined according to known dynamics important in the formation, transformation and spreading of the main water masses that circulate in the upper, intermediate and deep layers. The climatological characteristics of temperature and salinity reflect the water mass structures and the general thermohaline circulation patterns. Spatial and temporal variations on a seasonal basis of nutrients and principal biological parameters are described along with some aspects of the trophic conditions of the Mediterranean Sea. The strongest signal of variability is along the vertical; however, horizontal inhomogeneities are mostly associated with the internal dynamics. The distribution of the biochemical elements, in conjunction with hydrographic measurements of temperature and salinity, may serve as appropriate tracers for the characterisation of the main water masses (Atlantic Water, Levantine Intermediate Water and Bottom Water in the eastern and eastern basins) throughout the Mediterranean Sea. In a first approach, adequate descriptors of water properties have been obtained, useful for the quality control of incoming data in large databases and in setting-up documented procedures to improve future data management practices. Secondly, the biochemical climatological characteristics addressed in this paper are verified to be consistent with the physics of the Mediterranean Sea and are conceived useful to initialise coupled physical–biological models. The full set of spatially averaged vertical profiles can be found and downloaded from the World Wide Web data server established at OGS (http://doga.ogs.trieste.it/medar/climatologies/).
© 2004 Elsevier B.V. All rights reserved.

Keywords: Mediterranean Sea; Hydrodynamics; Biochemical observations; Climatological fields; Marine ecosystem

* Corresponding author. Tel.: +39-40-2140201; fax: +39-40-2140266.
E-mail address: bmanca@ogs.trieste.it (B. Manca).

1. Introduction

The Mediterranean Sea is a semi-enclosed basin characterised by rough bottom topography with a narrow continental shelf (<200 m) and a steep continental slope (Fig. 1). The western and the eastern basins communicate through the relatively shallow Strait of Sicily and present peculiar topographic depressions characterised by great depths, where nutrient-rich deep-water masses are stored for long time. The most important depressions are the Algero-Provençal basin (maximum depth of ~2900 m), the Tyrrhenian Sea (~3900 m), the Ionian abyssal plain (~4200 m), and the Hellenic trench that runs from the Ionian into the Levantine basin (~5000 m); finally, in the Levantine basin, the deepest areas are the Rhodes depression (~4200 m) in the north and the Herodotus abyssal plain (~3000 m) in the south.

The Mediterranean Sea, located at mid-latitudes, is characterised by a rather sub-tropical climate with two well-defined seasons, winter and summer, and short periods of transition between them. It possesses an anti-estuarine thermohaline circulation and has an active water exchange with the northern Atlantic through the Strait of Gibraltar. As a consequence of the excess of evaporation over precipitation (~0.62–

1.16 m year^{−1}; Hopkins, 1978), Atlantic Water (AW) inflows at the surface and Mediterranean Water (MW) outflows along the bottom. In wintertime, outbreaks of cold and dry continental air masses lead to a significant negative heat budgets (~5–10 W m^{−2}; Castellari et al., 2000) and buoyancy losses, initiating deep and/or intermediate dense water formation. These events are recurrent over the shelf areas and in the offshore regions, both in the western and the eastern basins (MEDOC Group, 1970; Ovchinnikov et al., 1985; Malanotte-Rizzoli, 1991; POEM Group, 1992).

In a climatological sense, for physical and biogeochemical studies, the thermohaline circulation may be schematically described as follows (Robinson et al., 2001; Béthoux et al., 1992): (i) at the surface (0–150 m), relatively fresh AW (~36.5 psu) circulates from the Strait of Gibraltar to the easternmost part of the Levantine basin; (ii) in the intermediate layer (150–600 m), the saline Levantine Intermediate Water (LIW), regularly formed in the Levantine basin with a salinity of ~39.10 psu, spreads westwards and constitutes the non-returning flow towards the Strait of Gibraltar, and then into the Atlantic Ocean; (iii) in the deep layer, two internal thermohaline cells circulate dense water masses formed via convective events in the northern
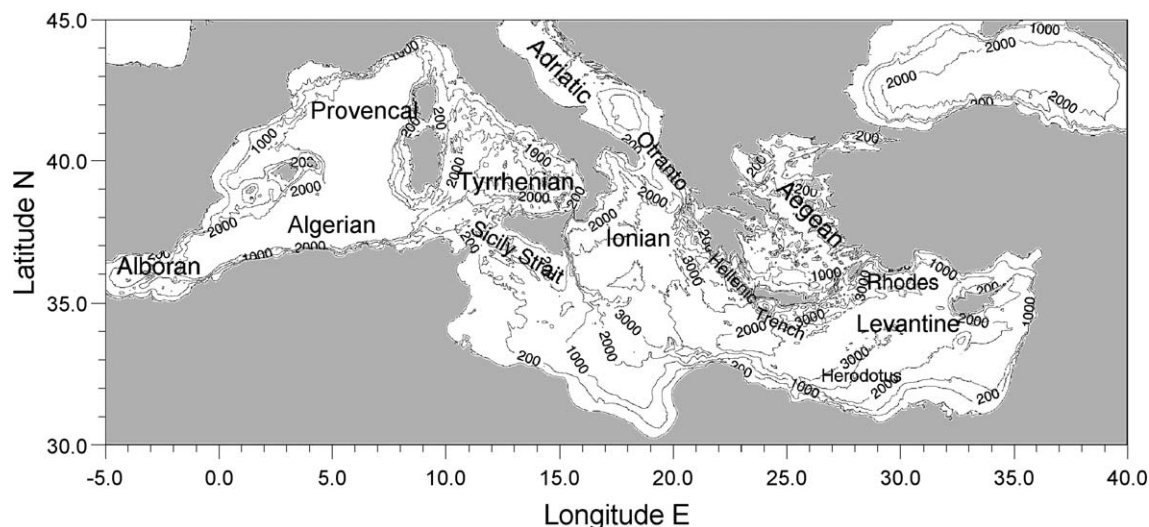

Fig. 1. Mediterranean Sea geography showing the names of the major sub-basins and the bottom topography. Depth contours are indicated in metres.

regions, mainly in correspondence to topographically controlled cyclonic gyres both in the Western and in the Eastern Mediterranean Sea. It has been generally accepted that the Western Mediterranean Deep Water (WMDW) forms in the Gulf of Lions (Leaman and Schott, 1991), and the Eastern Mediterranean Deep Water (EMDW) originates in the southern Adriatic Sea (Schlitzer et al., 1991). Transitional waters (i.e. between the intermediate and the deep layers) may be recognised everywhere as a product of the transformation of the intermediate and deep waters. These latter may participate in the outflow into the western basin through the Strait of Sicily (Sparnocchia et al., 1999; Astraldi et al., 2002), and into the Atlantic Ocean through the Strait of Gibraltar (Kinder and Parilla, 1987). Thus, the Mediterranean Sea influences, to a large extent, the global oceanic circulation (Reid, 1979).

Improvements in monitoring and numerical modelling have provided new insights into the general thermohaline circulation, which results much more complex than the one based on large-scale patterns. Atmospheric forcing and strong topographic constraints generate permanent and recurrent sub-basin scale cyclonic and anticyclonic motions. At the same time, the most energetic mesoscale activities play a major role in enhancing the internal dynamics and mixing processes (Millot, 1991; Robinson et al., 1991). In addition, seasonal characteristics and interannual variations of the circulation elements, verified by model simulations (Roussenov et al., 1995; Pinardi et al., 1997), affect the distribution of the biochemical species such as dissolved oxygen and nutrients, as well as the magnitude and the composition of phytoplankton biomass (Crise et al., 1999).

It has been demonstrated that the Mediterranean Sea is in a non-steady-state situation. A marked long-term warming trend and salinity increase in the deep water of the Western Mediterranean has been detected since 1960, i.e. from the period when the accuracy of the observations have revealed differences significantly greater than possible instrumental errors. These variations have been mostly attributed to changes in climate (Béthoux et al., 1990). These trends have been estimated to be about 0.027 °C and 0.019 units per decade in temperature and salinity, respectively (Leaman and Schott, 1991). However, since most of the

water transformation occurs during winter by convective events with a large participation of the LIW, these trends have been also related to an increase in the LIW properties due to man-induced reduction of the freshwater inflow for agricultural purposes (Rohling and Bryden, 1992).

Most dramatically, hydrographic observations conducted over the last decade in the Eastern Mediterranean have revealed a major transition event, due to an additional source of dense waters established in the Aegean Sea (Roether et al., 1996). More saline, warmer and denser waters ($S \cong 38.85$, $\theta \cong 13.80$ °C, $\sigma_\theta \cong 29.22$ kg m^{-3}; Klein et al., 1999) than the EMDW of Adriatic origin ($S \cong 38.66$, $\theta \cong 13.30$ °C, $\sigma_\theta \cong 29.18$ kg m^{-3}; Schlitzer et al., 1991), flowing out through the Cretan Arc Straits, sank to the bottom layer of the central Mediterranean regions, replacing almost 20% of the dense water below 1200 m. This event, named as Eastern Mediterranean Transient (EMT), has been attributed to an important meteorological anomaly that occurred in the Eastern Mediterranean at the beginning of the 1990s (Lascaratos et al., 1999). Changes in the distributions of salt (Malanotte-Rizzoli et al., 1999) and of the biogeochemical materials have also been observed in the intermediate and deep layers of the Eastern Mediterranean (Klein et al., 1999).

Many projects have produced significant amounts of multidisciplinary hydrographic data both in the Western and the Eastern Mediterranean Sea, i.e. MEDIPROD (Coste et al., 1972), PRIMO (Millot, 1995), POEM (Robinson and Malanotte-Rizzoli, 1993), ALMOFRONT 1 (Prieur and Sournia, 1994), EROS 2000 (Martin and Milliman, 1997), EU/MAST/MTP (Lipiatou et al., 1999), MTP II/MATER (Monaco and Peruzzi, 2002). Individual hydrographic experiments were specifically designed to investigate physical processes and the impact on nutrients and biological production. Nutrient enrichment has been observed at the surface in the presence of convective chimneys in the Gulf of Lions (Coste et al., 1972), in the southern Adriatic gyre (Gacic et al., 2002) and during severe winters in the area of the northern Levantine occupied by the cyclonic Rhodes Gyre (Yilmaz and Tuğrul, 1998); whereas low nutrient values have been detected in the neighbouring anticlones (Kress and Herut, 2001). In the upper layer, nitrate concentrations are higher in winter than

in summer, when oxygen rich and very low nutrient surface waters are rapidly capped creating conditions of high oligotrophy in the subsurface layer. Differences in nutrient concentration and changes in biodiversity between the Eastern and Western Mediterranean, due to the different physiography of the two interconnected basins, have been verified from a fully coupled physical and biochemical cycling model (Crise et al., 1999). The inverse estuarine circulations cause a net loss of nutrients in the eastern and western basins through the Sicily and the Gibraltar Straits, respectively (Béthoux et al., 1992).

In this paper, the most complete data set of archived historical data collated within the framework of the EU/MEDAR/MEDATLAS II and the basin-scale measurements obtained from the EU/MTPII/MATER project have been used. Since the data sets cover the interval from the beginning of the last century to the present, these data are analysed to calculate climatological profiles on a seasonal basis and to characterise the main water masses, providing a basis for describing their spatial variability. The same profiles can be used for checking the quality of historical and incoming data from operational oceanography, as well as for the initialisation of coupled hydrodynamical–biological models and sensitivity analyses.

The main purpose of the study is to deduce physical properties and biochemical characteristics of the principal water masses, taking into account vertical transfers and the general thermohaline circulation. This is done by analysing the vertical climatological profiles of temperature, salinity, dissolved oxygen, primary nutrient elements (nitrate, phosphate, silicate) and chlorophyll-*a*, calculated in different regions of the Mediterranean Sea. It should be stressed that the dissolved oxygen, nutrient and chlorophyll-*a* values have been employed merely as straightforward descriptors of the spatial and temporal variability of the water column structure, without any consideration of the underlying biochemical processes that are involved. The biochemical properties, although non-conservative have been used in the past to get supplementary information on the water masses (Coatanoan et al., 1999); the non-conservative aspects of these properties will not be discussed in the present study, but will be the object of future investigations into the functioning of the Mediterranean marine ecosystem.

The paper is organised as follows: in Section 2, we assess the quantitative content of the hydrographic data mentioned above and the quality control adopted within the framework of the data management practices. In Section 3, the data distributions and the statistical analyses performed to deduce the climatological characteristics of the physical and biochemical properties in the different regions of the Mediterranean Sea are described. In Section 4, we present typical climatological vertical profiles for some regions in the western and eastern basins. Some scientific frameworks are discussed analysing the results with emphasis on the properties of the most significant water masses circulating in the Mediterranean Sea. The concluding remarks of the present work are summarised in Section 5.

2. Data sets

2.1. Data archived within EU/MEDAR/MEDATLAS II and EU/MTP II/MATER projects

Earlier efforts in collecting historical data sets and mapping climatological fields in the Mediterranean Sea include those of Miller et al. (1970), Levitus (1982), Guibout (1987), Picco (1990) and Levitus et al. (1998). The twin EU/MAST/MODB and MEDATLAS projects provided quality controlled data sets of temperature and salinity in the Mediterranean Sea and produced an updated version of the horizontal climatologies and combined error field estimates (MODB Group, 1996; MEDATLAS Consortium, 1997).

The EU/MEDAR/MEDATLAS II project has improved the volume of available physical data and extended the database to include some biological and geo-chemical parameters in the Mediterranean and Black Seas (MEDAR Group, 2002). The project involved the majority of the scientific institutions of the bordering countries, thereby obtaining the best coverage of biochemical data in the whole Mediterranean. The core parameters comprise hydrographic data relating to temperature, salinity, dissolved oxygen, seawater nutrients (nitrates, phosphates and silicates), pH, alkalinity and chlorophyll-*a*.
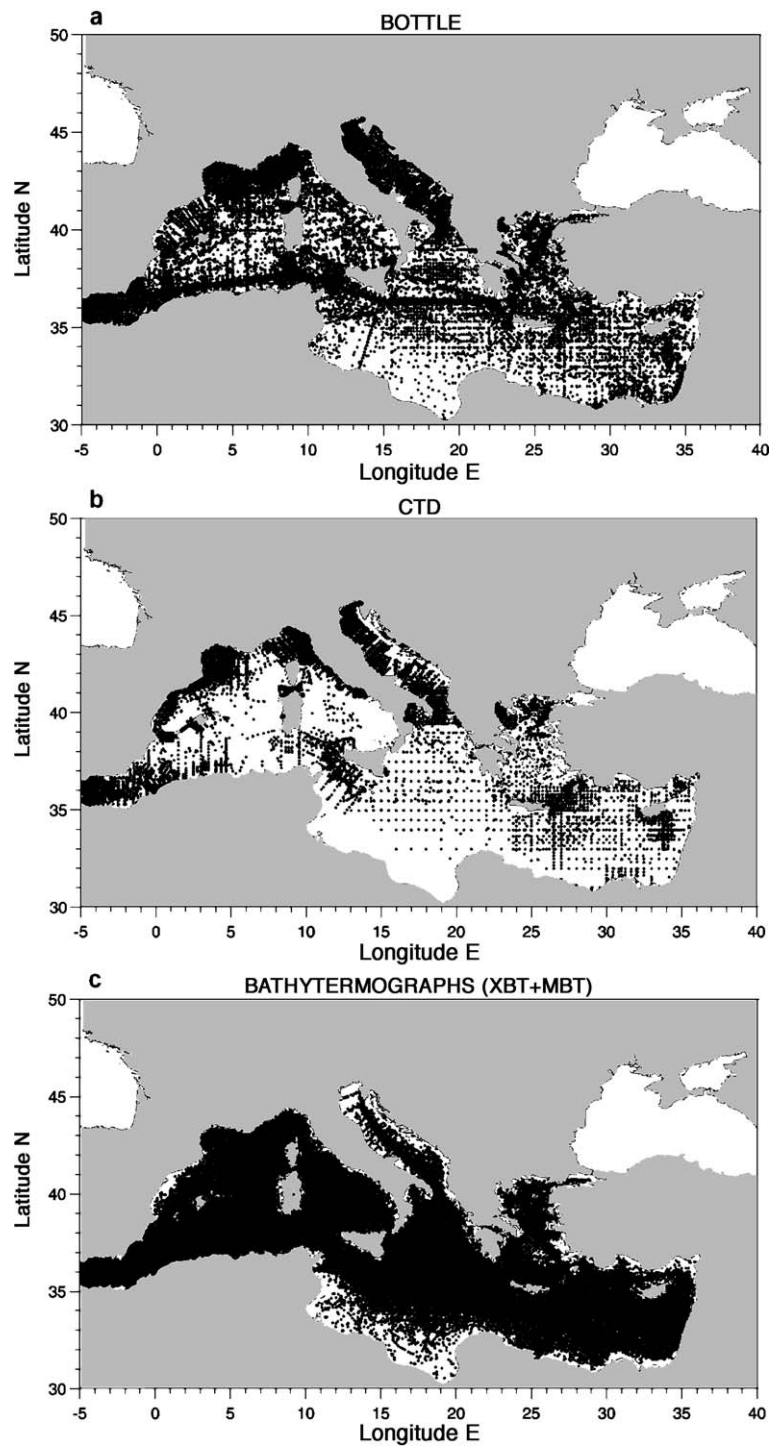
Fig. 2. Maps showing the locations of the hydrographic stations globally assembled in the MEDAR/MEDATLAS II database: (a) bottle casts (Nansen/Niskin), (b) CTD casts, (c) MBT and XBT probes.

The MEDAR/MEDATLAS II database consists of 286,397 vertical profiles, including bottle, CTD, MBT and XBT casts. Fig. 2 illustrates the distribution of the hydrological stations by data type, while Fig. 3 shows the distribution per year. Despite the good coverage of the Mediterranean Sea, the space and time distributions of the considered parameters are rather heterogeneous. The bottle stations display a fairly regular coverage of the western and eastern basins, with the exception of the southern coastal region in the Eastern Mediterranean, but the majority of them contain temperature and salinity data, exclusively. The CTD stations cover the period from the early seventies onward (Fig. 3), providing a major concentration in some regions of the Mediterranean Sea. The temperature and salinity profiles obtained with CTD probes reach down to the bottom layer and are useful to detect small variations of the temperature and salinity

fields. In contrast, the MBT and the XBT profiles extend vertically to a depth of about 250 and 700 m, respectively. These measurements, being less accurate (~ 0.1 °C) than the conventional measurements obtained by reversing thermometers (~ 0.02 °C) and CTD probes (~ 0.005 °C), can capture the seasonal variability in the upper thermocline or changes in the intermediate layer only in the presence of significantly strong dynamics.

Together with the historical MEDAR/MEDATLAS II database, the most recent data set collected in limited areas of the Mediterranean Sea within the framework of the MTP II/MATER project has also been considered (Maillard et al., 2002). The EU/MTP II/MATER database deals with an additional 3141 CTD profiles, 634 XBT probes and 1327 bottle casts of multidisciplinary biochemical samples collected during a series of oceanographic cruises
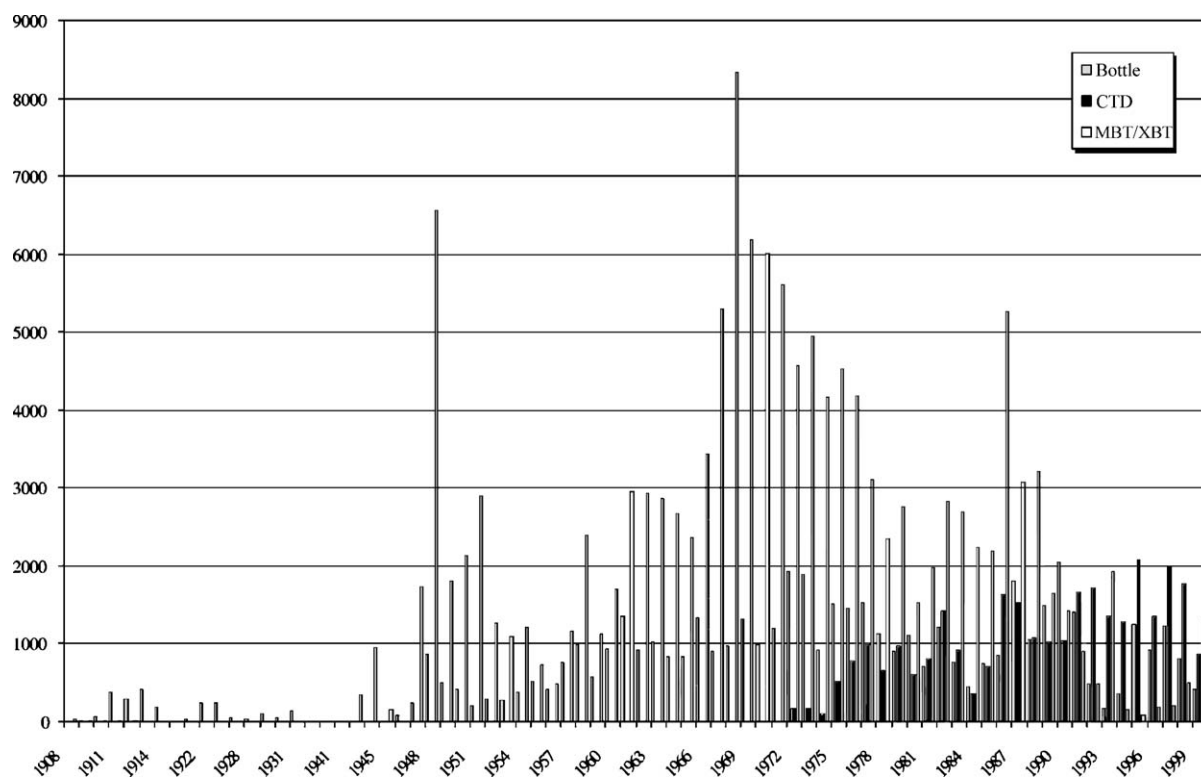

Fig. 3. Temporal distribution of the hydrological stations since the beginning of the last century that were used for the climatological analyses: CTD (black scale), bottles (grey scale) and bathythermographs (white scale).

from 1996 to 1999. It provides for the first time a good resolution in the vertical distribution of oxygen and nutrients (nitrate, phosphate and silicate) in the Algerian basin, in the Strait of Sicily and in the southern Adriatic. Hydrographic bottle casts were collected also in the Ionian Sea, in the Levantine basin and in the Aegean Sea.

The quantity of hydrological casts analysed in this work, i.e. with the exclusion of the stations pertinent to the Black Sea and the adjacent region in the Atlantic Ocean (Fig. 2), is synthesized in Table 1. The overall distributions of hydrological stations (Nansen/Niskin bottles, CTD, XBT and MBT) for temperature, salinity, dissolved oxygen, nutrients (nitrate, phosphate, silicate) and chlorophyll-*a* in the Mediterranean Sea used to reconstruct the spatially averaged vertical profiles addressed in this work are shown in Fig. 4. The density of hydrological stations decreases from North to South; the distribution of casts with chlorophyll-*a* measurements shows that the large majority of the data is located in the Western Mediterranean (along the Catalan, Spanish and Algerian coastlines) and in the Adriatic Sea; few stations cover the offshore regions in the Eastern Mediterranean.

2.2. Data quality control within MEDAR/MEDATLAS II project

The data quality control adopted within the MEDAR/MEDATLAS II data management work was based on specific protocol (Maillard et al.,

Table 1
Number of hydrographic stations globally assembled for the Mediterranean Sea within the framework of the MEDAR/MEDATLAS II and MTP II/MATER projects that were used for the climatological analyses

Data type	Data sets no.	Profiles no.	Period
Bottle	1633	52,068	1908–1999
CTD	561	29,663	1970–1999
MBT and XBT	894	141,110	1908–1999
Total	3088	222,841	

Bottle cast parameters are depth, temperature, salinity, oxygen, phosphate, nitrate, nitrite, ammonium, silicate, pH, alkalinity, and chlorophyll-*a*.
CTD cast parameters are depth, temperature, salinity and sometimes, oxygen.

2001) designed according to international methods and standards (UNESCO, 1993). The procedure was as follows: (i) data and metadata (ancillary information) are checked and reformatted in a unique format, (ii) numerical checks are performed by the comparison of the incoming data with prescribed ranges (e.g. broad ranges values) and reference statistics (e.g. spatially averaged vertical profiles and standard deviations), and (iii) the behaviour in the water column and the acceptability of consecutive values are checked testing the hydrostatic stability and searching for spikes and artefacts. Successively, a quality flag is added to the station header (meta-data information), and to each of measured numerical values also.

The temperature and salinity data have been fully quality checked in this way. For the biochemical data, a preliminary analysis of the major sources of existing data was performed to determine broad range values, which could then be confidently used to qualify incoming data from historical or unknown field investigations.

The major difficulty in the process of data validation arises from the fact that the marine environment exhibits some trends and/or interannual variations. The incoming data might or might not fit the existing climatologies (MODB Group, 1996; MEDATLAS Consortium, 1997; Levitus et al., 1998), which are representative of the mean and variance of the oceanographic fields but is time-independent. Consequently, the model for data validation described above may fail and trend evaluations should be included to improve the methods for data quality control. However, these requirements are quite difficult to fulfil due to the scarcity of systematic information and the lack of long time series in many areas. Therefore, the final action of flagging inconsistencies was decided visually and corrected manually, i.e. subjectively, to account for quality control flags that may be incorrect due to the characteristics of the used climatologies, which might not be adequately representative. The data with quality flag 1 (i.e. good data) and quality flag 2 (i.e. outside one standard deviation of the used climatologies) were retained for the following analyses. From the total number of profiles that were available for each parameter (Table 1), we finally retained about 99% of the temperature, 98% of the
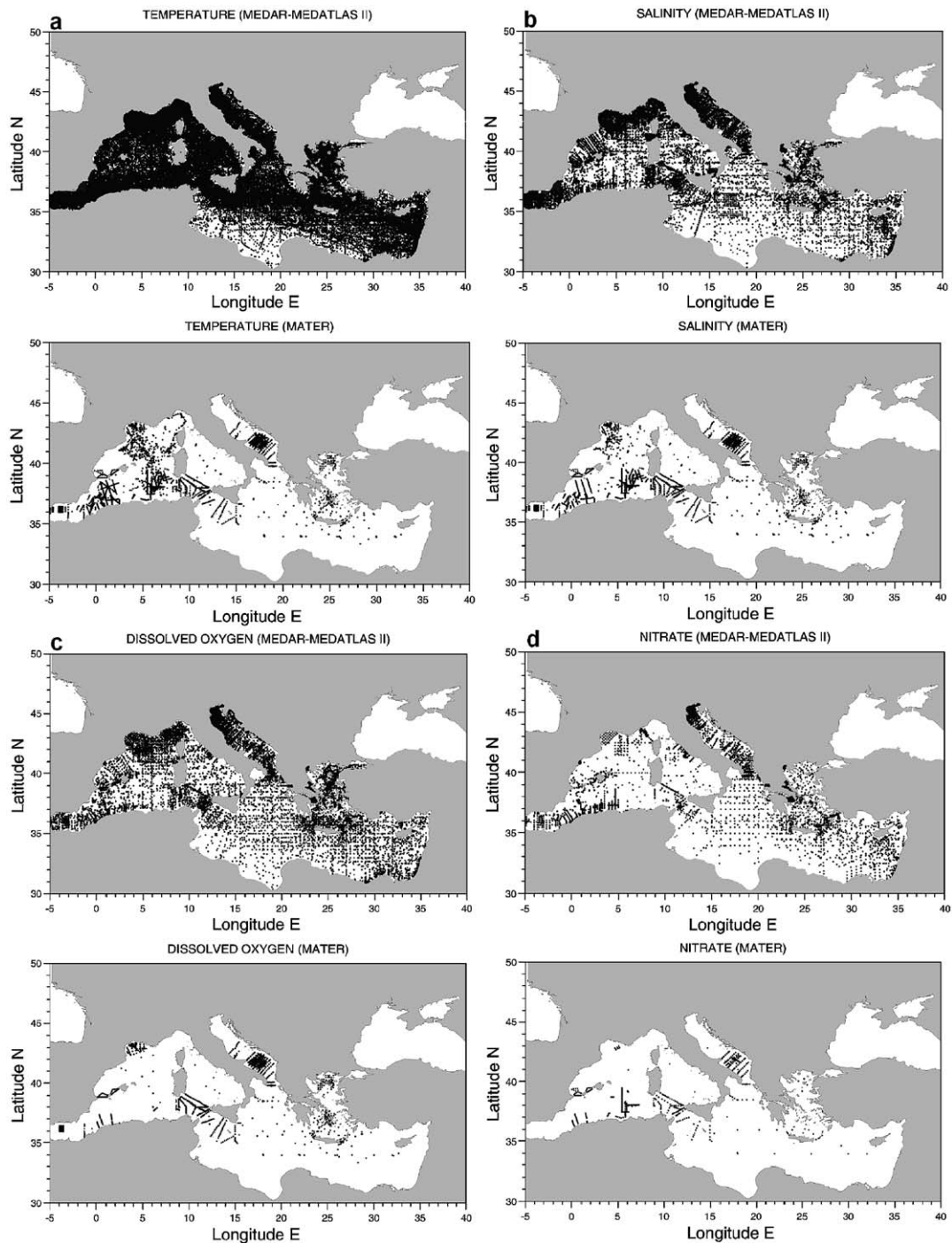
Fig. 4. Distribution of sampling stations originated in the context of the EU/MAST/MEDAR-MEDATLAS II and EU/MTPII/MATER projects for (a) temperature, (b) salinity, (c) dissolved oxygen, (d) nitrate, (e) phosphate, (f) silicate, and (g) chlorophyll-*a* used to reconstruct the averaged vertical profiles addressed in this work.
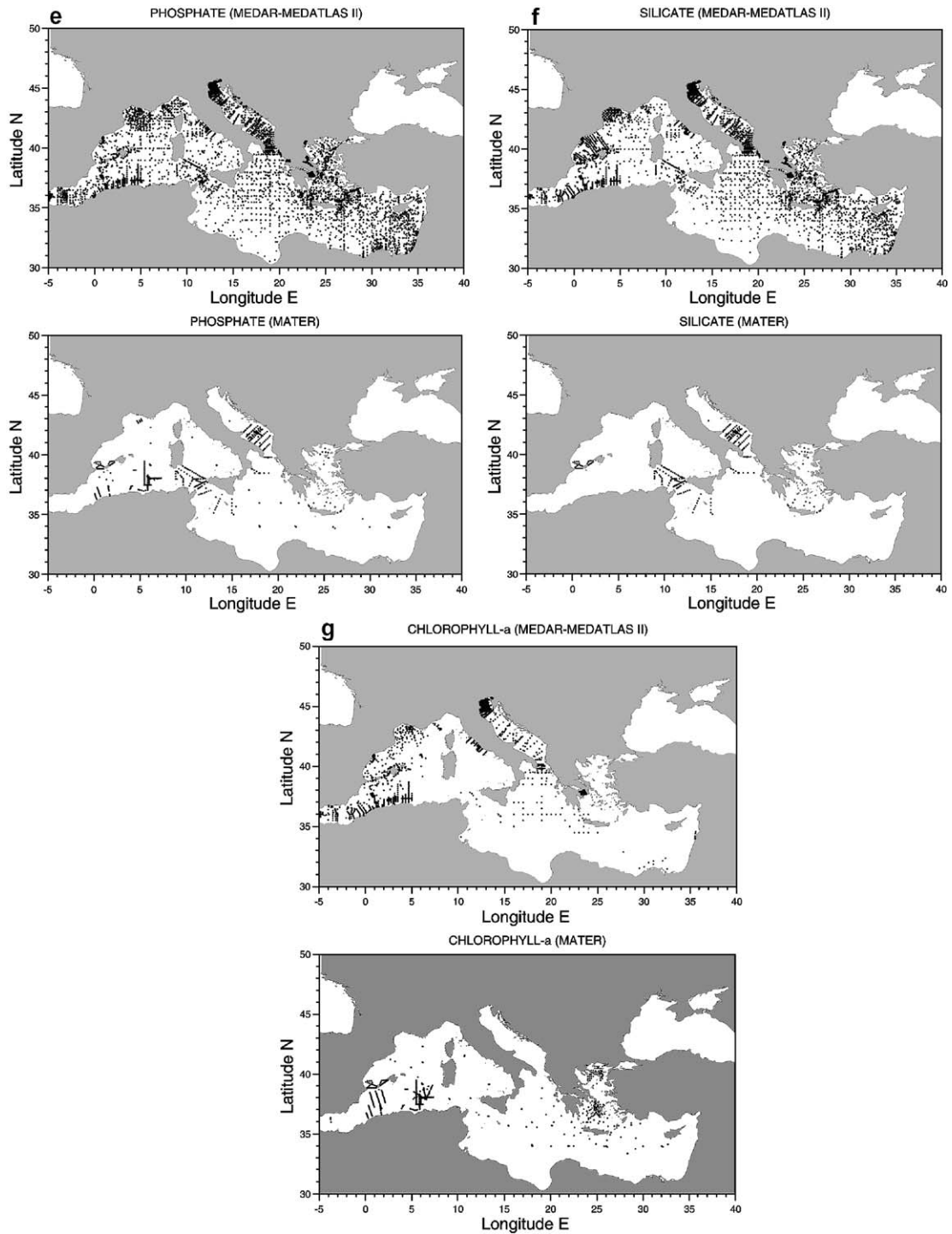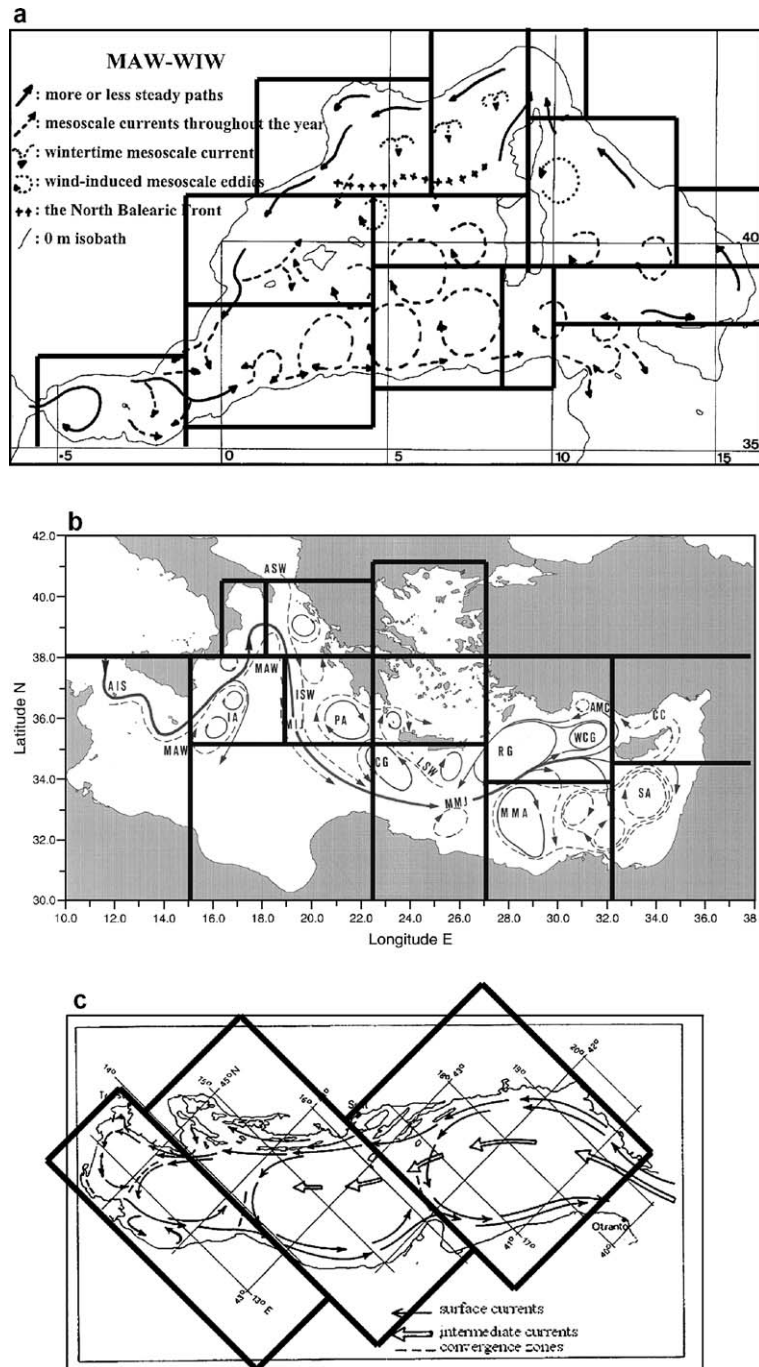
Fig. 4 (*continued*).

Fig. 5. Mediterranean regions defined according to the schematic representation of the upper thermohaline circulation in (a) Western Mediterranean (redrawn from Millot, 1999), (b) Eastern Mediterranean (redrawn from Robinson et al., 1991; Malanotte-Rizzoli et al., 1999) and (c) Adriatic Sea (redrawn from Mosetti, 1983).

salinity, 97% of the dissolved oxygen, 94% of the nitrate, 98% of the phosphate, 97% of the silicate, and 98% of the chlorophyll-*a* profiles.

3. Methods of analysis

3.1. Mediterranean regions defined according to general circulation patterns

Detailed hydrographic surveys conducted during the last two decades have assessed reliable schemes of the sub-basin scale thermohaline circulation and water mass pathways. Mesoscale phenomena have been traced by means of fragmentary evidence from specific surveys. Some gaps still exist, specifically over large areas in the southern regions of the Eastern Mediterranean. However, the dynamics in the regions have been recently filled with complementary information from model simulations and satellite images (Wu and Haines, 1998; Marullo et al., 1999). The schemes shown in Fig. 5 roughly represent the typical permanent features in the upper layer (0–200 m). On the basis of these schemes, the Mediterranean Sea has been subdivided into sub-regions (Fig. 5), which exhibit typical features (e.g. regions mostly affected by convective mixing vs. other regions where advective processes prevail). Fig. 6 and Table 2 summarise the nomenclatures used in the text and the basic physiography of the sub-regions defined above. It should be stressed that the utilised circulation diagrams represent the upper sub-basin scale dynamics, exclusively. One may consider that the two deep/internal thermohaline cells in the western and eastern basin certainly possess larger scale features; therefore, the above sub-regions oversample the deep dynamics and they can be also considered to characterise the spatial variability that affect the deep layers.

3.2. Spatially and seasonally averaged vertical profiles at standard depths

Spatially and temporally averaged vertical profiles of physical and chemical parameters (i.e. temperature, salinity, dissolved oxygen, nitrate, phosphate, silicate and chlorophyll-*a* concentrations) were constituted considering hydrological casts within the above-defined regions, separately and over seasonal periods. Table 3 summarises the total amount of hydrological stations available in each region and for each considered parameter to conduct the present analysis. Thirty-four standard levels (0, 5, 10, 20, 30, 40, 50, 75, 100, 125, 150, 200, 250, 300, 400, 500, 600, 700, 800, 900, 1000, 1100, 1200, 1300, 1400, 1500, 1750, 2000, 2500, 3000, 3500, 4000, 4500, 5000), which resemble the major standard levels defined in the Climatological Atlas of the World Ocean (Levitus et al., 1998) and in the MEDAR/MEDATLAS II protocols (Maillard et al., 2001), were defined to obtain more accurate "images" of the water column structure.
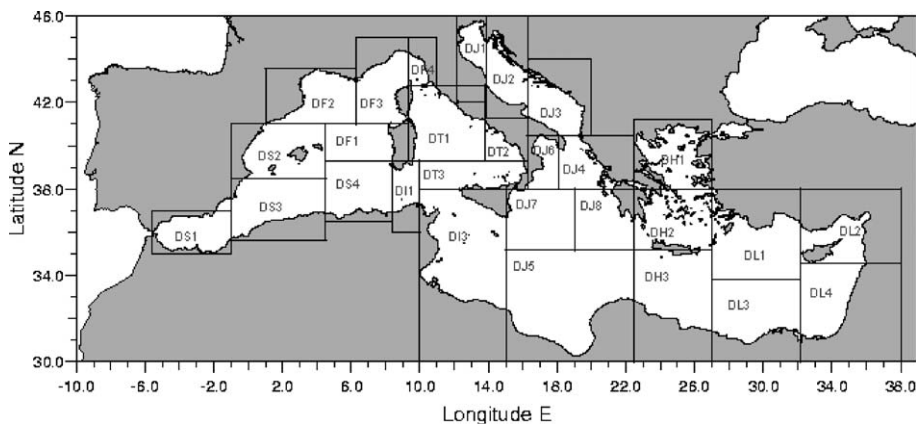

Fig. 6. Map of the Mediterranean Sea showing the geographical limits and the nomenclatures of the regions defined in Fig. 5 (cf. Table 2).

Table 2
Geographic limits and basic physiography of the Mediterranean regions defined according to the schematic thermohaline circulation features (cf. Fig. 5)

Code	Region	Lat N (min)	Lat N (max)	Lon E (min)	Lon E (max)	Depth (m)	Volume (km^3)
Western Mediterranean							
DF2	Gulf of Lions	41 00′	43 36′	01 00′	06 18′	2642	117,629
DF3	Liguro-Provençal	41 00′	45 00′	06 18′	09 18′	2791	151,632
DF4	Ligurian East	42 48′	45 00′	09 18′	11 00′	1146	3592
DS2	Balearic Sea	38 30′	41 00′	−01 00′	04 30′	2653	105,501
DF1	Algero-Provençal	39 18′	41 00′	04 30′	09 18′	2791	140,658
DS1	Alboran Sea	35 00′	37 30′	−05 36′	−01 00′	2583	48,954
DS3	Algerian West	35 36′	38 30′	−01 00′	04 30′	2728	208,249
DS4	Algerian East	36 30′	39 18′	04 30′	08 24′	2799	209,205
DT1	Tyrrhenian North	39 18′	42 48′	09 18′	13 48′	3991	185,963
DT2	Tyrrhenian East	39 18′	41 18′	13 48′	16 16′	3451	26,888
DT3	Tyrrhenian South	38 00′	39 18′	10 00′	16 16′	3446	114,422
DI1	Sardinia Channel	36 00′	39 18′	08 24′	10 00′	2529	24,477
DI3	Sicily Strait	30 00′	38 00′	10 00′	15 00′	1611	54,624
Eastern Mediterranean							
DJ1	Adriatic North	42 00′	46 00′	12 10′	13 50′	63	548
DJ2	Adriatic Middle	41 18′	46 00′	13 50′	16 16′	258	4344
DJ3	Adriatic South	40 36′	44 00′	16 16′	20 00′	1211	24,425
DJ6	Ionian North–West	38 00′	40 30′	16 16′	18 05′	2758	36,387
DJ4	Ionian North–East	38 00′	40 30′	18 05′	22 30′	3647	75,994
DJ7	Ionian Middle West	35 10′	38 00′	15 00′	19 00′	3991	290,358
DJ8	Ionian Middle East	35 10′	38 00′	19 00′	22 30′	4653	239,530
DJ5	Ionian South	30 00′	35 10′	15 00′	22 30′	3949	422,804
DH1	Aegean North	38 00′	41 12′	22 30′	27 00′	1747	23,088
DH2	Aegean South	35 10′	38 00′	22 30′	27 00′	4424	72,987
DH3	Cretan Passage	30 00′	35 10′	22 30′	27 00′	4007	264,455
DL1	Levantine North	33 50′	38 00′	27 00′	32 10′	4227	291,136
DL2	Levantine North–East	34 35′	38 00′	32 10′	38 00′	2452	47,918
DL3	Levantine South	30 00′	33 50′	27 00′	32 10′	3133	238,281
DL4	Levantine South–East	30 00′	34 35′	32 10′	38 00′	2650	116,332

The months allocated to each season were as follows: January–March for winter, April–June for spring, July–September for summer, and October–December for autumn. Vertical temperature, salinity and dissolved oxygen profiles were computed seasonally for the entire water column in all the Mediterranean regions, while for nutrients seasonal means were considered reliable for the first 0–200 m and annual means in the layer below. However, in some regions where the winter convection may play a major role in vertical water column homogenisation, as in the Gulf of Lions, in the Adriatic Sea and in the Rhodes gyre area, the amount of the available data allowed us to calculate seasonal profiles over the entire water column.

The observed levels for each hydrographic cast were converted to the standard depths using a weighted parabolic interpolation method (Reiniger and Ross, 1968). The final composition of the climatological profiles included the averaged vertical profiles along with the relevant computed standard deviation. In order to avoid the influence of extreme and possibly erroneous values or large biases derived from the coastal stations, the statistical analysis was reiterated once. After computing primary means and standard deviations, the data departing from the mean by more than one standard deviation, in absolute value, were rejected. The rejected data were less than 20–30% of the total measurements. The graphic representation of the

Table 3

Total number of hydrological casts used to calculate the spatially averaged vertical profiles of TEMP=temperature, PSAL=salinity according to the practical salinity scale, DOX1=dissolved oxygen, NTRA=nitrate, PHOS=phosphate, SLCA=silicate, and CPHL=chlorophyll-*a*, in the different regions of the Mediterranean Sea (data from CD-ROMs MEDAR/MEDATLAS II, 2002 and MTP II/MATER, 2001)

Code	Region	TEMP	PSAL	DOX1	NTRA	PHOS	SLCA	CPHL
Western Mediterranean								
DF2	Gulf of Lions	13,859	12,625	10,517	4998	6498	11,613	11,955
DF3	Liguro-Provençal	16,800	16,380	12,281	15,345	12,350	12,650	11,739
DF4	Ligurian East	3254	3180	3127	38	1288	498	0
DS2	Balearic Sea	7768	7523	6296	4937	4710	6484	6497
DF1	Algero-Provençal	3694	3641	3499	2053	2507	2455	2536
DS1	Alboran Sea	15,374	14,235	10,361	9148	10,304	9687	10,578
DS3	Algerian West	11,909	9482	6150	7456	7318	6642	9797
DS4	Algerian East	7670	6417	4250	4253	4199	2739	4023
DT1	Tyrrhenian North	10,495	10,386	9172	7026	8622	6508	1059
DT2	Tyrrhenian East	1475	1470	1231	0	822	0	0
DT3	Tyrrhenian South	7804	6662	5784	4573	4705	4472	10
DI1	Sardinia Channel	4134	3640	2784	1176	1681	1162	3
DI3	Sicily Strait	10,410	9934	9557	8545	8513	8398	6951
Eastern Mediterranean								
DJ1	Adriatic North	8253	8169	6129	5896	5406	6129	638
DJ2	Adriatic Middle	4832	4721	2868	2581	2451	3323	428
DJ3	Adriatic South	7379	6906	4611	4041	4193	4079	1230
DJ6	Ionian North–West	1834	1670	1591	597	795	597	0
DJ4	Ionian North–East	4023	3848	3624	2998	3150	3233	1156
DJ7	Ionian Middle West	17,226	16,694	13,727	13,386	13,347	14,196	5
DJ8	Ionian Middle East	7608	7078	7035	6007	6007	5610	7
DJ5	Ionian South	5953	5879	5832	4496	4464	3777	25
DH1	Aegean North	6784	6362	6144	4183	4950	4717	3014
DH2	Aegean South	10,558	10,230	10,100	9737	9777	9580	5549
DH3	Cretan Passage	8353	8256	8148	7826	6119	7871	14
DL1	Levantine North	7992	7698	7650	5794	6791	5436	22
DL2	Levantine North–East	1640	1636	1642	932	933	1181	0
DL3	Levantine South	5312	5159	5156	2410	3280	4089	1434
DL4	Levantine South–East	9151	9136	8941	6563	7107	6418	5081
Total		221,544	209,017	178,207	146,995	152,287	153,544	83,751

spatially averaged vertical profiles of dissolved oxygen and nutrients, as shown in the following, have been obtained after a three-point "running average" smoothing filter.

4. Results and discussion

4.1. Western Mediterranean regions

The spatial variability in the Western Mediterranean is discussed by comparing the averaged vertical profiles in three regions: the Gulf of Lions (region-DF2), the Tyrrhenian Sea (region-DT1) and the Algerian basin (region-DS4).

The Gulf of Lions is mainly characterised by a permanent cyclonic circulation and manifests strong seasonal variations of the physical and biochemical properties (Fig. 7) due to convective movements and deep mixing during the wintertime. The seasonal thermocline extends to a depth of 50 m in summer (Fig. 7a); it is deeper in autumn reaching down to 100 m. In summer, stratification conditions and the prevailing northwesterlies allow the spreading of the less saline AW (Fig. 7b) transported by the Ligurian Current (Millot, 1999). In winter, the deep convection sets the homogenisation of the water column (Fig. 7a) bringing saline water from the intermediate layer close to the surface (Fig. 7b). Typical values indicate a salinity increase of about $\Delta S = 0.55 \pm 0.32$ at the sur-
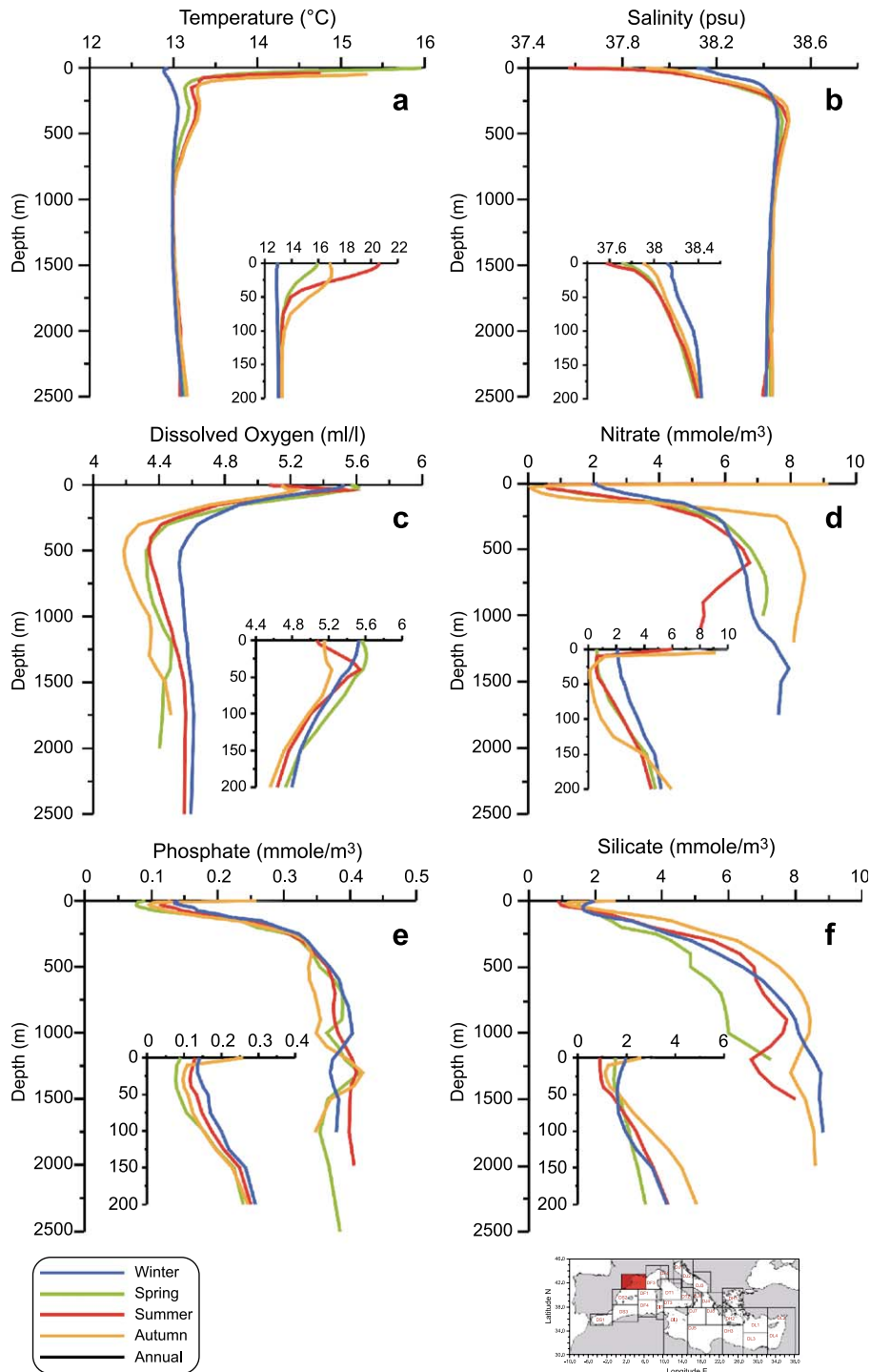
Fig. 7. Seasonally averaged vertical profiles of (a) temperature, (b) salinity, (c) dissolved oxygen, (d) nitrates, (e) phosphates, and (f) silicates in the NW region of the western Mediterranean (DF2—Gulf of Lions). The insets indicate the shallower portion of the profiles.

face and ΔS=0.16$\pm$0.09 at a depth level of 100 m; on the contrary, the salinity decreases ($\sim$0.04$\pm$0.03) in the LIW layer, which occupies the 200- and 800-m depth interval.

Similar patterns also appear in the oxygen and nutrient profiles (Fig. 7c–f). In winter, a rather high ventilation (oxygen content>5.4 ml l^{-1}) and enrichment of nutrients ($\sim$2.1 mmol m^{-3} for nitrate and $\sim$0.14 mmol m^{-3} for phosphate) is evident in the upper water column, whilst an almost nutrient depleted layer is established in summer and autumn. In summer, the upper water column is topped by relatively low-oxygen layer; a shallow oxygen maximum located at 40–50 m retains the same concentration as in winter. However, biological activity cannot be neglected, and the oxygen increase derives from the general phytoplankton bloom that occurs at the beginning of spring (Coste et al., 1972). Nutrients are consumed between winter and summer and phosphates appear utilised more rapidly. During the stratification period, the highest nutrient concentrations appear at the surface and sharply decreases to a depth of about 5–10 m; this is clearly due to the Rhone river discharge that constitutes the major runoff to the western basin (Béthoux et al., 1992). The permanent nutricline is well established at 100–150 m during the stratification seasons, whilst it moves upward to the base of the euphotic zone in winter. Deep waters reveal an oxygen minimum (O_2 $\sim$4.2–4.6 ml l^{-1}) at about 500 m associated with the LIW layer; below this layer, abnormally high nutrient concentrations (NO_3=8.1 mmol m^{-3}; PO_4=0.40 mmol m^{-3}; Si=8.5 mmol m^{-3}) result from terrestrial inputs, and from the mineralization processes related to the oxidation of the organic matter precipitating from the euphotic zone (Béthoux et al., 1992).

Seasonally averaged vertical profiles of temperature and salinity in the Algerian basin and in the Tyrrhenian Sea are depicted in Figs. 8 and 9, respectively. The temperatures in the upper water column display similar behaviour in the two regions over the entire annual cycle. In summer, the surface waters are essentially stratified and attain the same temperature values; in the winter months, the thermocline disappears almost completely leading to the formation of a vertically homogenised water column down to the bottom; the surface temperatures reach climatological values of $\sim$14.0 °C in the Tyrrhenian Sea and $\sim$14.5

°C in the Algerian basin. Note also the strong north–south gradient, considering the very low climatological value of $\sim$13 °C in the northern convection region (Fig. 7a). The salinity profiles reflect the advective explanation of salinity changes in the Western Mediterranean given by Millot (1999); it is mainly dictated by the westward propagation of Atlantic water, which results relatively fresher in the Algerian basin than in the Tyrrhenian Sea.

In the intermediate layer, the water column structures between 250 and 750 m emphasise the presence of relatively high temperature and salinity values indicating the LIW. These features are much more pronounced in the Tyrrhenian basin (Fig. 9) than in the Algerian basin (Fig. 8), in agreement with the circulation pattern of the LIW schematically depicted by Millot (1999) in his Fig. 2. However, in the Tyrrhenian Sea the LIW properties change during the year displaying a maximum of salinity in autumn. In winter, the salinity in the LIW core decreases (Fig. 9b) due to the vertical mixing in the nearly permanent cyclonic gyre (Sparnocchia et al., 1994).

Hydrographic properties in the deep part of the Tyrrhenian Sea (Tyrrhenian Deep Water—TDW) exhibit higher climatological temperature and salinity values ($\Delta t \sim 0.17$ °C; $\Delta S \sim 0.04$) than those observed for the WMDW at the formation site. These results are in agreement with the observations of Sparnocchia et al. (1999), which indicated that significant amounts of Eastern Mediterranean transitional and deep waters flow through the Strait of Sicily below the LIW into the Tyrrhencuian basin where they sink and mix with the ambient Western Mediterranean waters.

Fig. 10 addresses the spatial variability of the hydro-chemical properties in the Western Mediterranean, showing the differences between the annually averaged vertical profiles for the three regions mentioned above. The purpose of this analysis is to assess the role of the upper/external and the deep/internal 'conveyor belts' in defining the biochemical characteristics of the water masses throughout the Western Mediterranean. The oxygen minimum layer is found at $\sim$500 m and it is more pronounced in the Algerian basin, in agreement with the decrease in the salinity of the LIW core, because more time is needed for the LIW to flow into the Algerian basin after its recirculation in the Tyrrhenian Sea. In the layer below, the oxygen content shows more pronounced positive
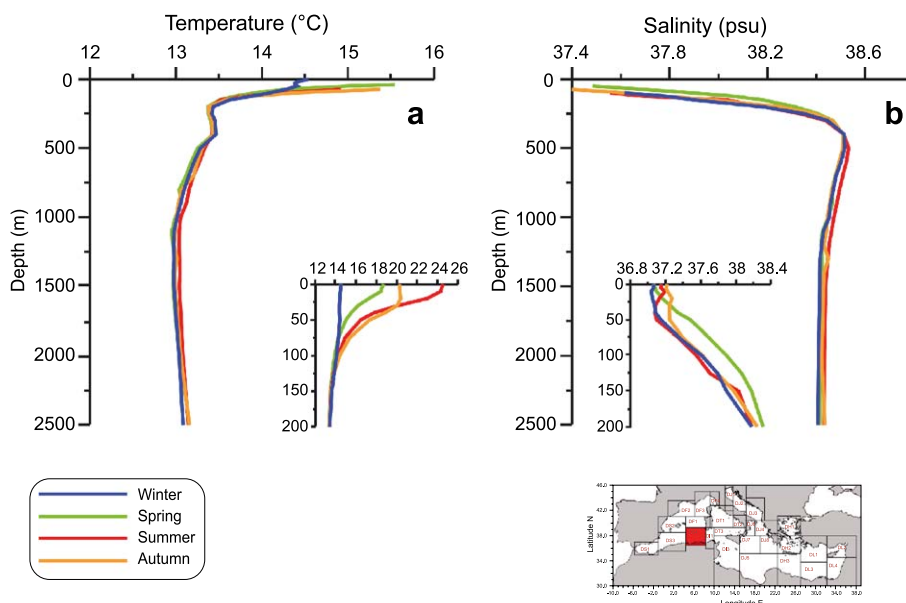
Fig. 8. Seasonally averaged vertical profiles of (a) temperature, and (b) salinity in the southern region of the western Mediterranean (DS4—Algerian basin). The insets indicate the shallower portion of the profiles.

anomalies in the northwestern basin, indicative of the region prone to the deep convection. The WMDW formed there moves into the Algerian basin and then into the Tyrrhenian Sea. The profiles of nutrients (Fig.

10b–d) exhibit remarkable spatial variations. The upper waters overlying the permanent nutricline (<200 m) are generally poor in nutrients; however, their values are higher in the Gulf of Lions. In the
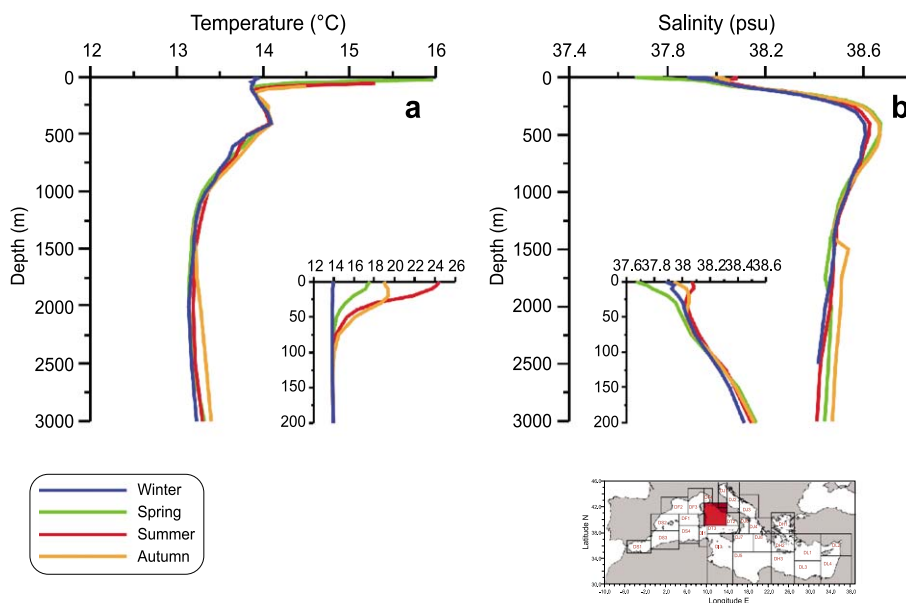

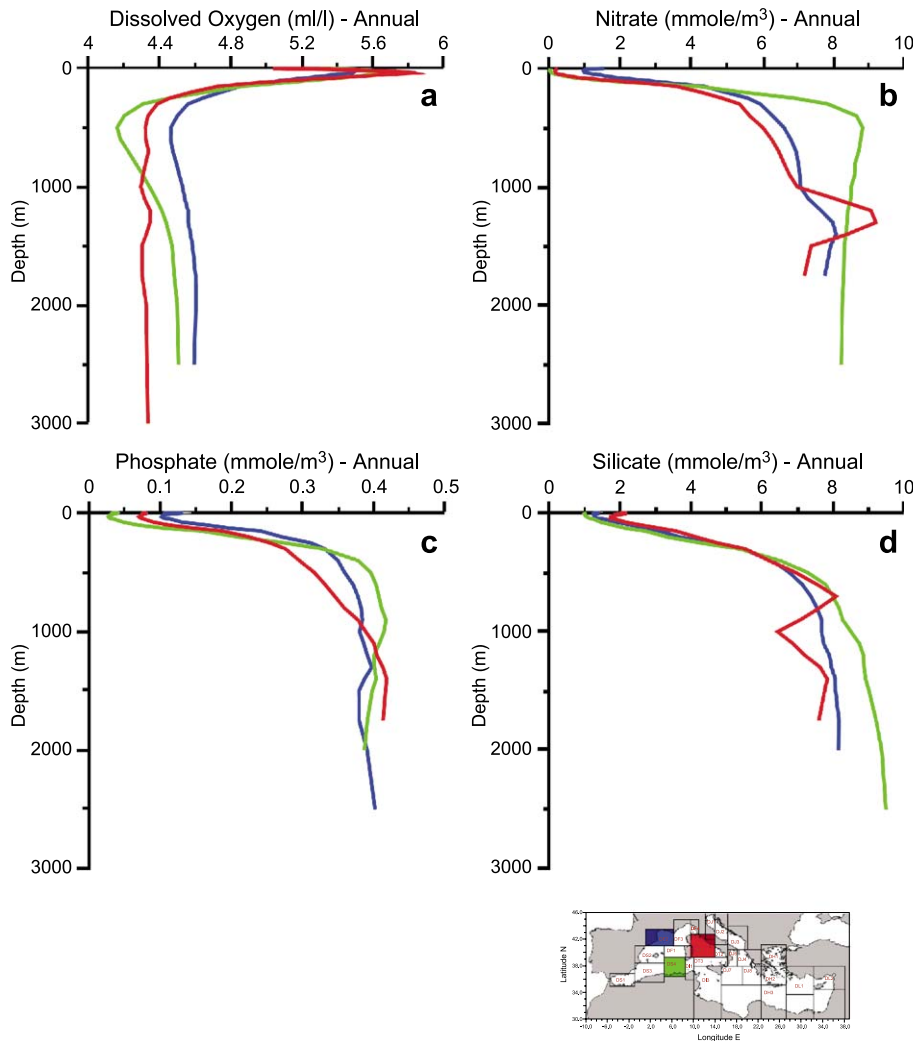Fig. 9. As for Fig. 8 but for the Tyrrhenian Sea (DT1).

Fig. 10. Superimposed annually averaged vertical profiles of hydrographic parameters for selected regions (see inset map) in the western Mediterranean: (a) dissolved oxygen, (b) nitrate, (c) phosphate, and (d) silicate.

other regions, the photic zone exhibits lower nutrient concentrations, close to the detectable limits, generally attributed to phytoplankton consumption and the scarce supply of nutrient-rich waters from the deep layer. The vertical profiles of nutrients are almost mirror images of those of the dissolved oxygen. The high spatial variability mostly reflects the advective process of the involved water masses. The highest values of nitrate and phosphate concentrations (Fig. 10b and c) are at ∼ 500 m, i.e. at the same depth of the oxygen minimum, and are higher in the Algerian basin than in other areas. These features may elucidate

some questions raised by many authors about the preferential pathway of the LIW in the Western Mediterranean (Millot, 1999; Sparnocchia et al., 1999); the climatological fields of the oxygen and nutrient concentrations confirm the results obtained from the analysis of the salinity profiles earlier. The silicates in the deep waters (>500 m) always exceed 7 mmol m^{-3} throughout the year (Fig. 10d). The highest values above 9 mmol m^{-3} in the Algerian basin imply long residence times and poor ventilation, whilst lower silicates (∼ 8 mmol m^{-3}) in the convection region are representative of the WMDW of more

recent formation. The poor estimates for this param-
eter in the deep Tyrrhenian basin are in large part due
to the lack of data in this region.

The chlorophyll-*a* data contained in the databases
are scarce and did not allow the elaboration of
seasonal profiles for all the regions in the Western
Mediterranean due to gaps in the spatio-temporal
distributions. In order to infer the seasonal variation,
we present the vertical profiles relative to the Gulf of
Lions (Fig. 11a), which exhibits strong differences
with respect to other regions, while Fig. 11b illustrates
the spatial variability among the three regions indi-
cated in the inset map during spring.

In the Gulf of Lions, the highest surface phyto-
plankton biomass develops in winter and spring due to
the violent mixing and vertical injections of nutrient-
rich deep waters in the open-sea convective region;
the vertical profiles also show sustained phytoplank-
ton activity at depth in winter, while during the rest of
the year, the depletion of dissolved inorganic nutrients
in the photic zone reflects low chlorophyll-*a* concen-
trations. In late winter and early spring, the phyto-
plankton growth is indicated in the subsurface waters,
as shown by the peaks of the chlorophyll-*a* maximum
at ∼ 10 m. Peak concentrations are found at depths of

50–70 m in summer and in autumn, the so-called
Deep Chlorophyll Maximum (DCM) typical of the
oligotrophic character of the Mediterranean Sea (Crise
et al., 1999), corresponding to the subsurface oxygen
maximum. The basic behaviour of the vertical chlo-
rophyll-*a* distribution, characterised by the presence
of the DCM, is also maintained in other regions (Fig.
11b). The vertical profiles shown in Fig. 11b refer
only to spring, since the database contains very little
chlorophyll-*a* data relating to the summer, and does
not contain any data at all for winter and autumn.
Away from the Gulf of Lions, the DCM seems much
weaker and deeper (∼ 50–75 m) and closely follows
the depth of the nutricline.

4.2. Eastern Mediterranean regions

4.2.1. The Adriatic Sea

The Adriatic Sea has been subdivided into three
sub-basins, which exhibit different general oceano-
graphic characteristics (Fig. 5c). A collection of an
unprecedented amount of hydrological data in the
Southern Adriatic Sea allows a more refined analysis
than that performed by Zavatarelli et al. (1998) of the
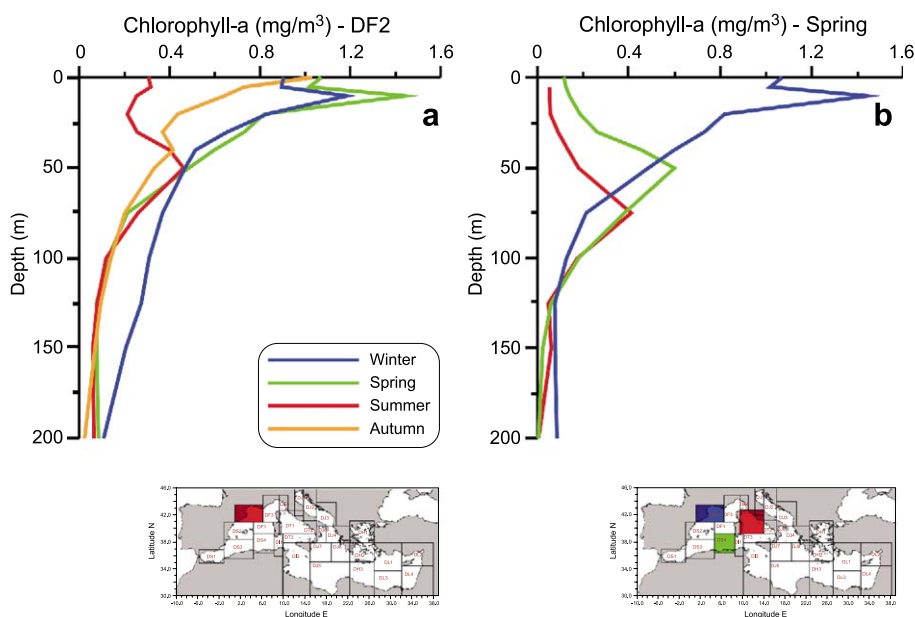seasonal variability of water mass structures and

Fig. 11. Superimposed averaged vertical profiles of chlorophyll-*a*: (a) seasonal variations in the Gulf of Lions; (b) spring climatology for the
regions indicated in the inset map.

biochemical properties. Fig. 12 shows the seasonally averaged vertical profiles of temperature, salinity, oxygen and nutrients in the southern region (DJ3). The temperature and salinity profiles (Fig. 12a and b) manifest a three-layer thermohaline structure. In the surface layer (0–150 m), the temperature profiles reflect basically the seasonal cycle. The surface waters are periodically exposed during wintertime to convective processes (Ovchinnikov et al., 1985) able to homogenise the entire water column to a temperature of ∼ 13.5 °C. In spring, the seasonal thermocline develops at approximately 75 m and extends to 100 m in summer. At the surface, an excess of the relatively fresh waters advected from the north sustains the very low static stability during winter months (Artegiani et al., 1997). The positive anomalies of temperature and salinity located between 100 and 400 m identify the LIW, which manifests its salinity maximum in autumn. The distinguishing feature in the deep layer is the decrease of temperature and salinity, which testifies either a large contribution of the cold and less saline (but dense) waters from the northern shelf in replenishing the deep trench in the Southern Adriatic Sea or a sufficient buoyancy loss of the less saline surface water during wintertime convection that would permit mixing to large depths.

The dissolved oxygen and nutrient profiles (Fig. 12c–f) display characteristics which result from the convection activity in this region during wintertime. In winter, more oxygenated water masses extend from the surface down to ∼ 600 m (Fig. 12c) due to the fast convective ventilation; in contrast, less ventilated and nutrient-rich (Fig. 12d–f) waters reside beneath. In summer, it seems that the contribution of oxygen from atmosphere is not able to overcome the biological consumption. The occurrence of pronounced subsurface oxygen maxima at a depth of about 30 m accompanied by the minimum nitrate values at the same depth are, however, mostly indicative of strong biological activity. Below 50 m, the concentrations show a strong gradient zone towards low values of dissolved oxygen and high values of nutrients. The nutrient enrichment in the intermediate and deep layers (Fig. 12 d–f) reflects the advection of the LIW (Civitarese et al., 1998), which manifests its maximum in autumn as in the case of the salinity values. In addition, contrary to the results showed by Zavatarelli et al. (1998), in large part due to the lack of

data, the convective mixing during winter has been demonstrated to be an important mechanism for the significant transfer of nutrients to the surface layer and the development of the spring phytoplankton bloom in the centre of the gyre (Gacic et al., 2002).

Interestingly, the oxygen profiles show in general an increase in the 800–1000-m depth interval during spring and summer periods accompanied by a decrease in the nutrients. This is an indication of freshly ventilated and dense waters advected from the northern shelf region rather than dense waters formed by convection to a depth greater than 600 m. These waters flow southwards driven by a bottom density current and may reach the southern latitudinal sections later in the year (Artegiani et al., 1997). There, having a density higher than the ambient water masses, they partly sink into the deep layer at the shelf break (Bignami et al., 1990; Manca et al., 2002) and partly flow against the continental slope. Both branches constitute the main component of the deep Adriatic outflow (ADW) over the sill depth (∼ 850 m) through the Strait of Otranto (Manca and Giorgetti, 1998). Subsequently, the ADW sinks into the adjacent Ionian Sea and fills the bottom layer of the Eastern Mediterranean (Schlitzer et al., 1991).

The bottom water in the southern Adriatic exhibits low oxygen and high nutrient values due to the longer residence time of this water mass in the deep trench at ∼ 1200 m. The silicates show a pattern similar to that of the other nutrients; the highest silicate values (∼ 10–15 mmol m^{-3}) imply a long residence time and poor ventilation.

4.2.2. The Ionian Sea

The Ionian Sea stands out as the region of the Eastern Mediterranean mainly characterised by the transit and transformation of the major water masses, i.e. the relatively fresh AW, the highly saline LIW and the colder and denser EMDW, which characterise the general thermohaline circulation in the upper, intermediate and deep layers, respectively (Malonotte-Rizzoli et al., 1997). In the Southern Ionian (region-DJ5, Fig. 6), the upper waters are mostly typified by the transit of the AW and the LIW that drive the well-known anti-estuarine circulation, whilst the properties of the deep waters are essentially determined by the deep/internal 'conveyor belt' driven by the dense waters of Adriatic origin. The spatially averaged deep
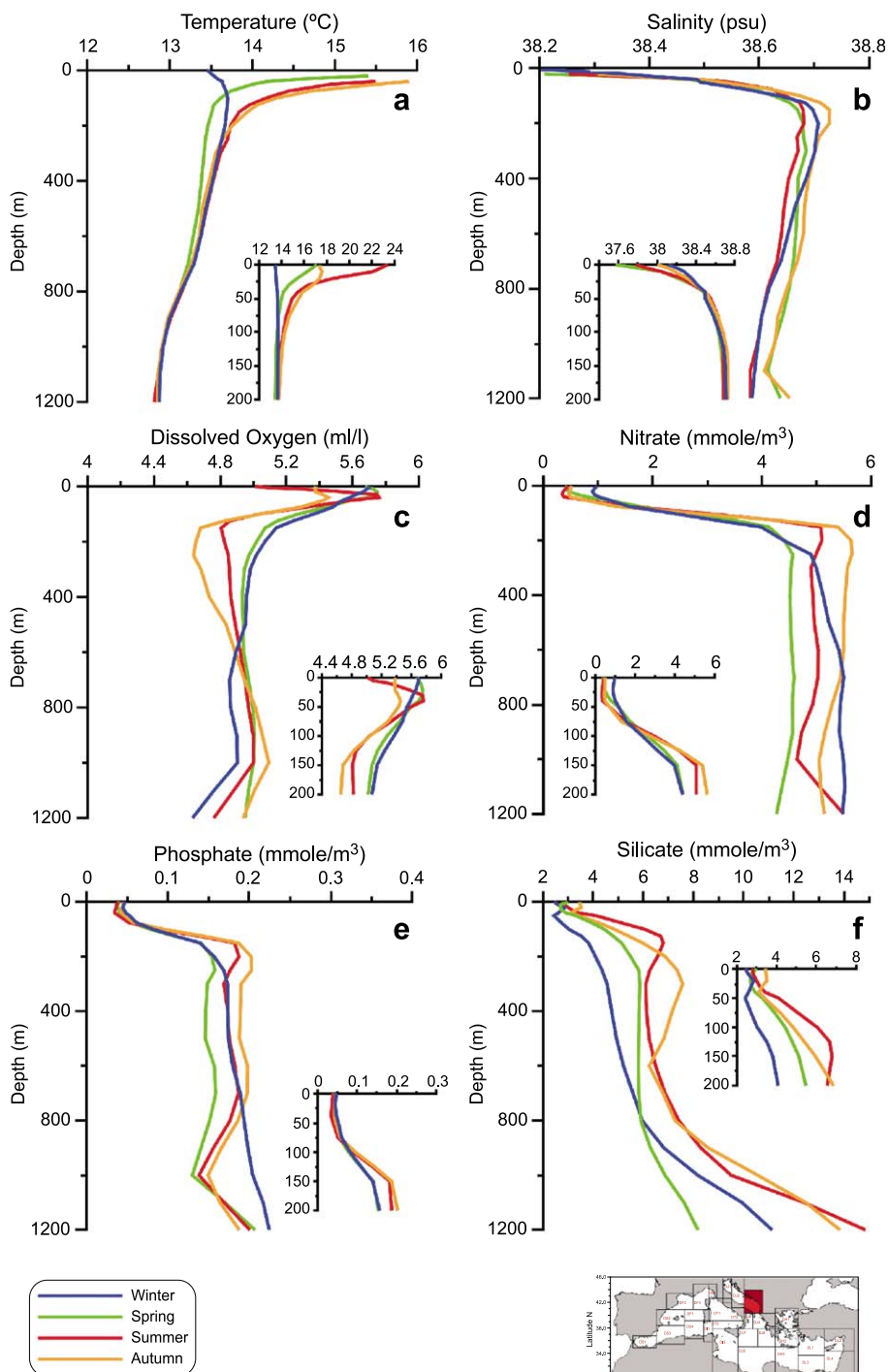
Fig. 12. Seasonally averaged vertical profiles of (a) temperature, (b) salinity, (c) dissolved oxygen, (d) nitrates, (e) phosphates, and (f) silicates in the southern Adriatic (DJ3). The insets indicate the shallower portion of the profiles.

profiles calculated from the data available in this region are shown in Fig. 13.

In the surface layer (0–150 m), the lowest salinity indicates AW that, after passing the Strait of Sicily, undergoes substantial modification along the way towards the Levantine basin. The seasonal thermocline extends down to 50–75 m (Fig. 13a); the most prominent feature appears during the stratified seasons when the excess of evaporation isolates less saline AW in the sub-surface layer at ∼50 m (Fig. 13b). Below 100 m, the water column exhibits almost permanent conditions of stratification mostly sustained by the sharp salinity gradient. The seasonal oxygen cycle (Fig. 13c) exhibits a subsurface maximum in summer and in autumn at about 50 m. The nutrient distributions (Fig. 13d and e) show that the photic layer is almost nutrient depleted throughout the year without appreciable seasonal variations indicating weak vertical mixing from the deep layer in winter months. However, the feeble mixing and ventilation processes occurring during the wintertime cause the nutrients to become available in the photic layer where they are quickly utilised in phytoplankton production processes that in the Ionian may occur rather early in the year (Napolitano et al., 2000). Moreover, the subsurface production has been seen in model simulations to occur below the thermocline also in June with a maximum of biomass in addition to that of the phytoplankton bloom in spring, giving conditions of higher oxygen concentrations and very low nitrate contents in the subsurface layer (Fig. 13c–e). The silicates (Fig. 13f) display some artefacts in the upper layer in winter and summer despite the selection of the data with specific quality flags, while in the other two seasons the profiles overlap, showing a behaviour that is very similar to those of nitrates and phosphates.

The intermediate layer is dominated by the LIW (∼200–600 m), typified by the salinity maximum that develops below the well-pronounced thermocline. The salinity in the LIW layer displays strong seasonal variability; in summer and autumn it spreads westward towards the Strait of Sicily purer than in the other seasons. The decrease of salinity manifests during the seasons prone to the mixing and it is certainly due to the vertical exchange with the less saline AW above. An upper limit of about 8 years has been estimated for the apparent travel time of LIW to the Strait of Sicily from CFC ages distribution (Roether et al., 1998). The water masses below the LIW layer (∼600–1200 m) present almost steady seasonal conditions, mostly characterised by the slow decrease of both temperature and salinity, due to the mixing of the LIW with the relatively fresh EMDW of Adriatic origin (Schlitzer et al., 1991). This layer, named the transitional layer in recent literature (Malonotte-Rizzoli et al., 1997), is mostly characterised by the 'oldest' water mass and the highest nutrient content, essentially due to a high oxygen consumption rate and very low convective renewal (Roether and Well, 2001).

In the deep layer, one would expect almost steady seasonal conditions with the exception of the convective regions; on the contrary, the more heterogeneous deep waters have multiple sources, which include the Adriatic, the Aegean and, on some occasions, the Rhodes Gyre region (Sur et al., 1992). The major complication in the assessment of the value of the temperature and salinity climatologies is the effect of the profound changes in the status of the Eastern Mediterranean which have occurred since the early 1990s (Roether et al., 1996). The large deviations below 1200 m, as shown in Fig. 13a and b, reflect water intrusions due to the EMT, and the seasonal variations depend on when the cruises were carried out.

Retrospective analyses of the historical deep profiles have been conducted by many authors (Özsoy and Latif, 1996; Lascaratos et al., 1999; CIESM, 2002) considering different regions in the Eastern Mediterranean, with the objective of distinguishing the climatic event and in particular with the attempt to identify further events that could have influenced the properties of the most important water masses in the past regime. In this study, the temperature and salinity data pertinent to the entire Ionian and Levantine basins were grouped separately in 1-year intervals since 1950 and volume-averaged in the depth interval from 1200 to the bottom (i.e. the deep layer mainly influenced by the transient event; Roether et al., 1996) to produce a time series. In Fig. 14, we illustrate the time sequence of the averaged potential temperature and salinity in the deep Ionian Sea. It is notable that, with the exception of some suspect values of salinity in terms of accuracy, the salinity field has fluctuated at least three times in the last 50 years, i.e. in the 1960s,
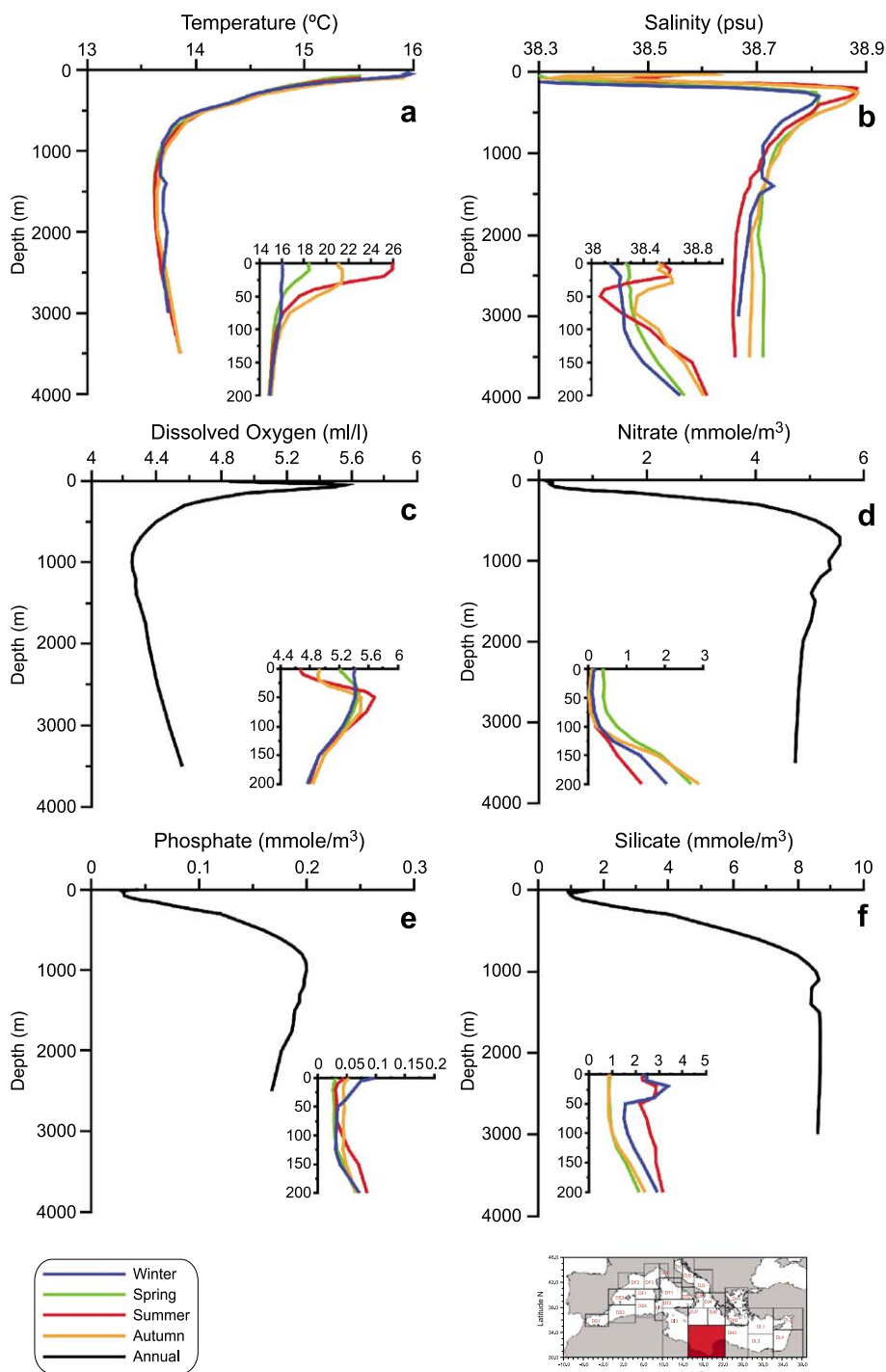
Fig. 13. Seasonally averaged vertical profiles of (a) temperature, (b) salinity. Annual-averaged vertical profiles of (c) dissolved oxygen, (d) nitrates, (e) phosphates, and (f) silicates in the southern region of the Ionian Sea (DJ5—South Ionian). The insets indicate seasonal variations in the shallower portion of the profiles.
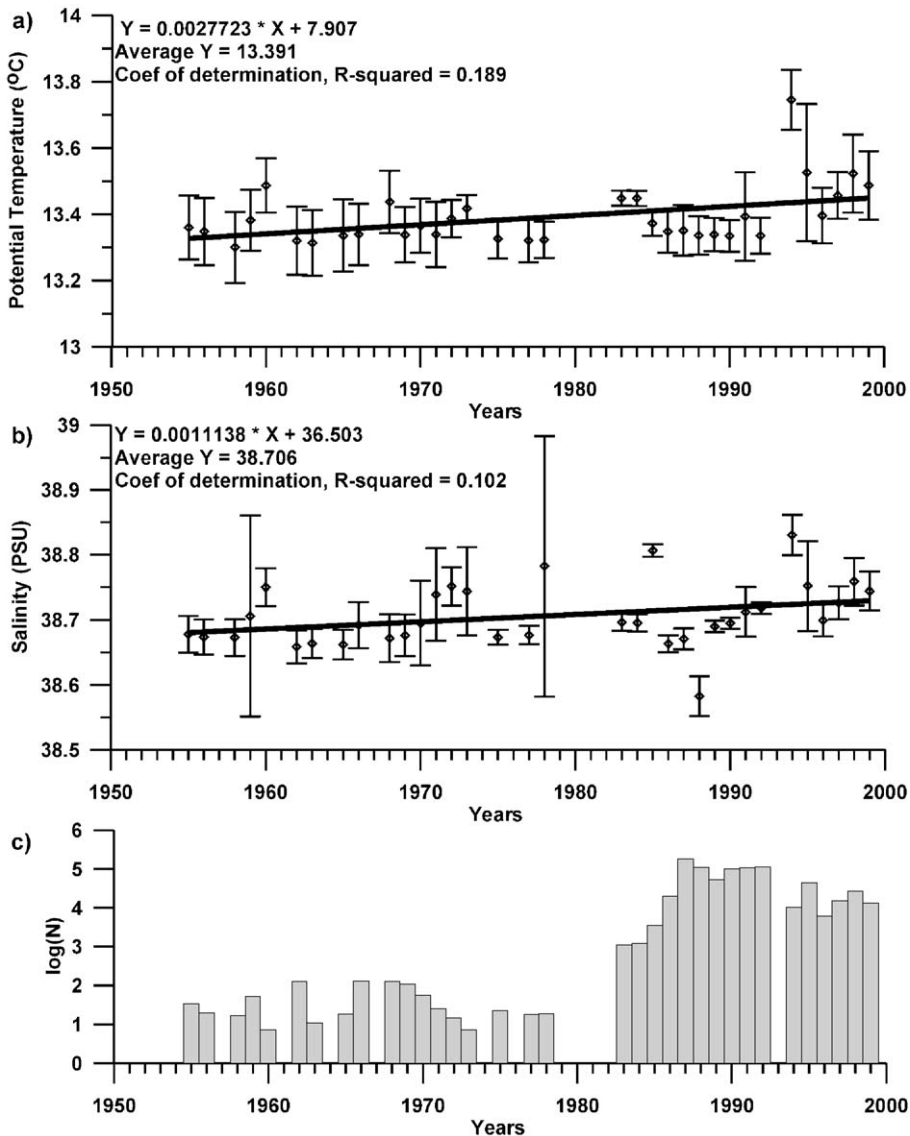
Fig. 14. Long-term changes in (a) potential temperature (°C) and (b) salinity. Number of data points (c) in the Ionian deep waters (>1200 m) obtained by grouping the hydrological profiles annually. The vertical bars denote one standard deviation confidence intervals. The linear regression lines and the r^2 correlation coefficients are indicated.

in the 1970s and in the 1990s, starting with the last increase in 1986. However, an overall trend of about 0.001 per year can be inferred for the salinity. The temperature shows a positive trend with an annual increment of about 0.003 °C per year. In order to reach firm conclusion in using the climatologies for future narrow range checks in the deep layer, we propose the combined use of seasonal climatologies

for the upper and intermediate layer, while the annual-averaged vertical profiles may be adopted for the deep waters; the actual climatological values can be further adjusted by trends.

4.2.3. The Levantine basin and the Rhodes gyre

A number of studies based on quasi-synoptic basin-wide surveys conducted in the Levantine basin
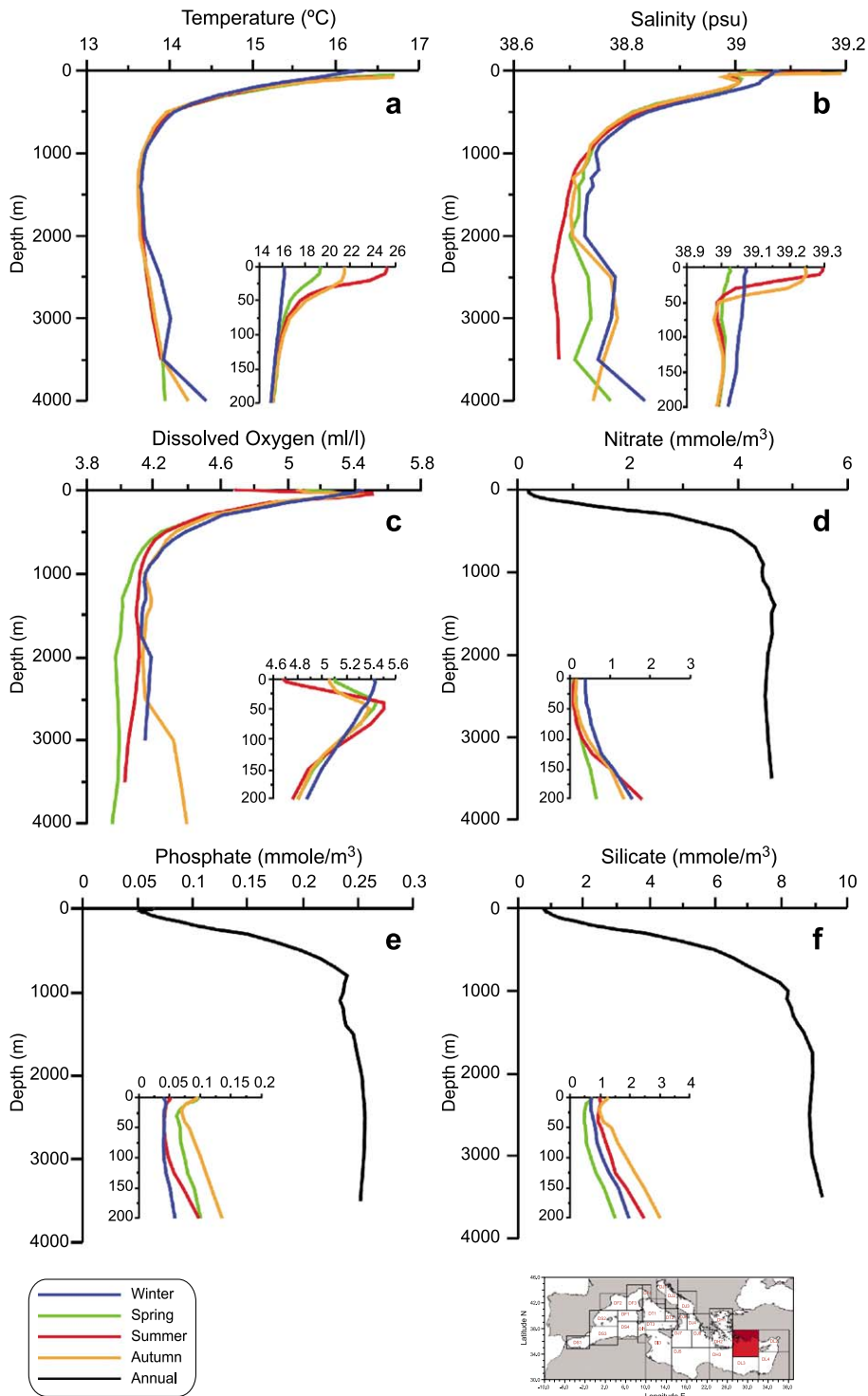
have shown that the thermohaline circulation is mainly characterised by a cyclonic region in the north and a series of anticyclones in the south (POEM Group, 1992 and Fig. 5b). In the northern cyclonic region, under prolonged winter conditions, the upper water column presents a well mixed layer which extends down to about 200 m. Typical isopycnals at surface are in the range of 29.00–29.05 kg m^{-3}; therefore, a moderate dense water forms, i.e. the LIW, regarded as the most important water mass of the Mediterranean (Özsoy et al., 1993). Deeper and more efficient mixing conditions were observed during severe winter leading to the formation of a variety of Eastern Mediterranean deep water, the Levantine Deep Water (Sur et al., 1992), which results warmer and saltier than the EMDW. In this region, during winter, the nutricline reaches the photic zone bringing relatively nutrient-poor deepwater masses close to the surface for biological consumption. These features in addition to a very limited external input of nutrients essentially make the Levantine basin one of the most oligotrophic regions of the Mediterranean (Yilmaz and Tuğrul, 1998). On the other hand, stratified conditions prevail in the southern region; under the influence of anticyclonic motion, the pycnocline deepens to ∼ 450 m, creating fairly constant distributions of high temperature, salinity and dissolved oxygen, and low nutrients (Krom et al., 1992). In the deep layer, no seasonal variations and spatial differences were noticed in nutrient concentrations, apart from a weak eastward oxygen decrease and silicate increase (Kress and Herut, 2001).

Fig. 15 depicts the climatological profiles in the northern region of the Levantine basin. In the upper layer, climatological temperatures span over a wide range from 16 to 25.5 °C (Fig. 15a). The salinities at the surface reflect the conspicuous effect of the high evaporation rate, reaching values higher than 39.2 in summer and in autumn. During the warm seasons, the highly saline Levantine Surface Water (LSW) forms in the surface layer up to ∼ 50 m. In the layer below, a strong halocline exists between the LSW and the AW; the latter may be recognised

in the subsurface layer by the minimum of salinity (<39.0) at ∼ 75 m (Fig. 15b). In winter and spring, the salinity decreases due to winter mixing of the LSW with the less saline water of Atlantic origin that upwells in the Rhodes cyclonic gyre. However, most of the salt accumulated at the surface by strong evaporative processes is transferred into the layer below (0–500 m) due to the intensification of the Rhodes gyre and continuous water column overturning.

In the deep layer, below 1000 m, the large difference in the seasonal profiles of temperature and salinity mostly derives from the dense water of Aegean origin. As for the Ionian Sea, we investigated the evolution of the water mass properties in the deep Levantine basin (1200–bottom) by constructing time series of potential temperature and salinity from yearly volume-averaged vertical profiles (Fig. 16). Evidence of a warming trend and an associated salinity increase emerges from these analyses; however, the linear correlations were not significant. On the other hand, despite the larger error bars during the era of the bottle casts, two very distinct episodes of large fluctuations in salinity can be noted, i.e. in the 1960s and in the 1990s. The latter starts in 1987 as in the Ionian Sea. It has been speculated that, while the second episode in the early 1990s is clearly related to the EMT, the one which occurred in the early 1970s seems to originate in the Levantine basin where it has shown the maximum signal (Theocharis et al., 2002). In brief, the climatological characteristics of the physical properties (temperature and salinity) show seasonal differences that depend on the EMT. However, this may be largely due to the fact that a great part of the seasonal data were obtained from specific surveys conducted more recently, i.e. following the appearance of the EMT, whereas very little relevant data is available for the earlier years in the historical database. Therefore, for future application of the climatological profiles in data quality checks related to the deep waters in the Eastern Mediterranean, we propose the use of regional climatologies computed on an annual basis from the entire data set.

Fig. 15. Seasonally averaged vertical profiles of (a) temperature, (b) salinity, and (c) dissolved oxygen. Annually averaged of (d) nitrates, (e) phosphates, and (f) silicates in the NE region of the eastern Mediterranean (DL1—North Levantine). The insets indicate seasonal variations in the shallower portion of the profiles.

a)
Y = 0.0037364 * X + 6.018
Average Y = 13.409
Coef of determination, R-squared = 0.380

b)
Y = 0.0006274 * X + 37.472
Average Y = 38.713
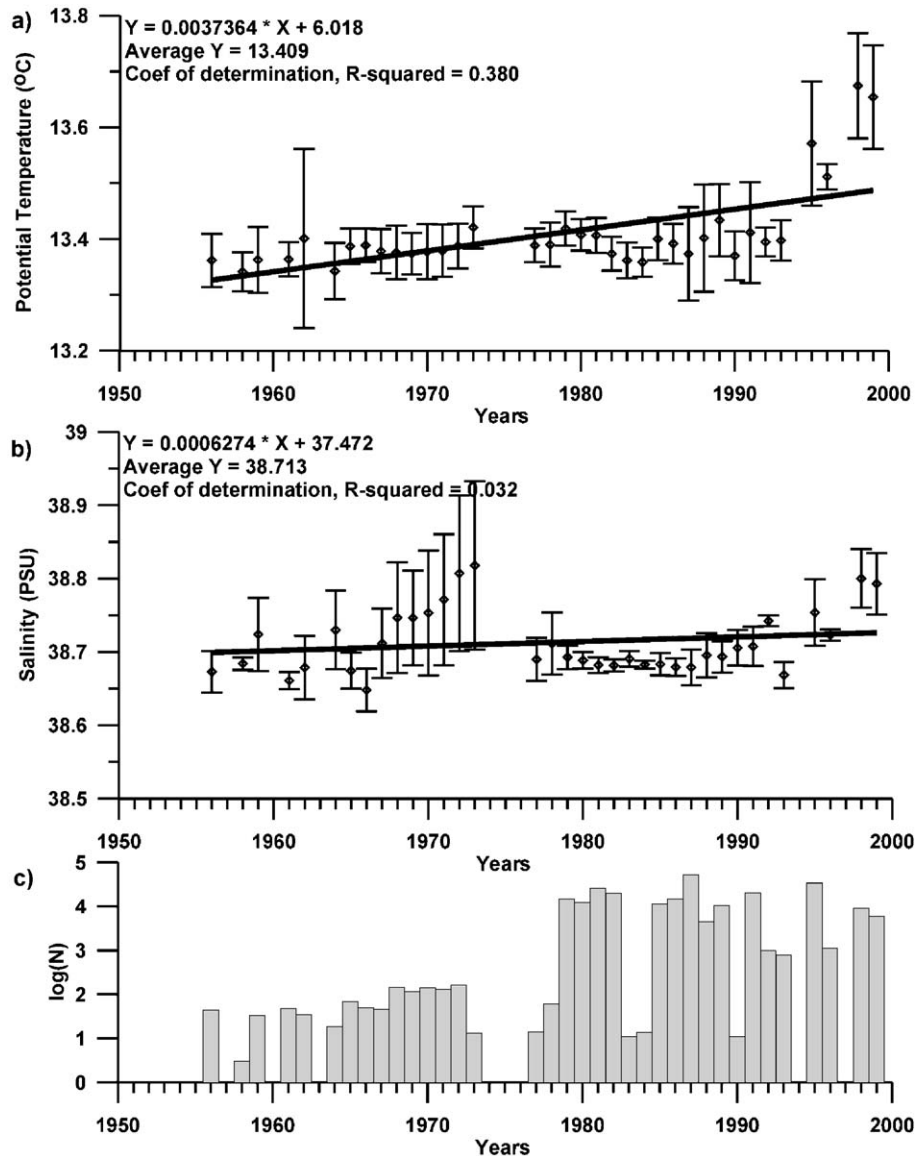Coef of determination, R-squared = 0.032

Fig. 16. As for Fig. 14 but for the Levantine basin.

Fig. 15c–f provides a general overview of the vertical distributions of oxygen and nutrients. In the upper layer, seasonal variations of the primary nutrient elements follow hydrographic features appropriate for a cyclonic region. In winter, the dissolved oxygen is of comparable magnitude as in other convective regions (e.g. the Gulf of Lions and the southern Adriatic gyre), emphasising the effect of the surface ventilation, whilst at depth, the observed profiles differ greatly with respect to other basins. During the stratified seasons, the concentrations present a shallow oxygen maximum at about 50 m, poor in nutrients due to photosynthetic consumption. A sharp nutricline essentially characterises the transition to the deep layer; the tendency of the nutricline to disappear during winter is less pronounced than in other convective regions. In the northern Levantine, the convective movements usually reach the intermediate

layer and a limited mixing with the nutrient-enriched and less saline deep waters occurs (Yilmaz and Tuğrul, 1998).

Spatial differences of biochemical properties distribution from west to east have been demonstrated by many authors on the basis of basin-wide climatological observations from earlier cruises (Miller et al., 1970). These differences indicate a longitudinal gradient of increasing oligotrophy in terms of phytoplankton production and stocks of biomass from the Ionian towards the easternmost part of the Levantine basin. Conceptual and statistically models applied to large quasi-synoptic databases (Denis-Karafistan et al., 1998) as well as coupled hydrodynamic–ecological model simulations (Crise et al., 1999) have reconstructed the East–West trophic gradient in the Mediterranean. Here, we are able to quantify the main spatial characteristic of trophic levels in the Eastern Mediterranean from vertical climatologies.

Fig. 17 shows composite profiles of oxygen, nutrients and chlorophyll-*a* calculated in three selected regions of the Eastern Mediterranean: two regions are in the northern and southern Levantine basin, and are mainly affected by cyclonic and anticyclonic eddies, respectively; the third region is in the Southern Ionian mainly characterised by lateral advection. The employed plotting method is useful to confirm the spatial differences among these regions due to different dynamics.

Some preliminary elements of the seasonal variability in the upper water column, mostly attributed to photosynthetic consumption, have been discussed above; here, some key elements of the spatial characterization of deep-water masses emerge from the comparison of the deep profiles which reflect different ecosystems and dynamics. In the deep layer, the dissolved oxygen concentrations decrease gradually from the Ionian towards the southern Levantine and are lowest in the northern Levantine (Fig. 17a). This is a clear manifestation of the spreading of the EMDW that has been supplied by the Adriatic inflow. In the Ionian, below a broad oxygen minimum at mid depths (~ 1000 m), the concentrations increase slightly towards the bottom indicating more ventilated bottom waters. This increase, still evident in the southern Levantine, disappears in the north where the deep convective mixing rarely extends

down to 1000 m in the Rhodes gyre (Özsoy et al., 1993), indicating a rather 'older' and stagnant situation in the deep layer.

Nutrient concentrations exhibit remarkable differences with depths and regions. The photic layer (~ 120 m) exhibits almost nutrient-depleted conditions; on an annual basis the photosynthetic consumption seems higher in the Levantine basin than in the southern Ionian. In the layer beneath, the nitrate concentrations increase sharply (Fig. 17b), reaching extreme values that result higher in the southern Ionian (~ 5.7 mmol m^{-3}) than in the Levantine basin (~ 4.7 mmol m^{-3}). This enhances the trophic gradient in the intermediate layer attributed to the spreading of LIW and subsequent export of nutrient-associated materials into the Ionian Sea. However, the enrichment of the LIW by nitrate as it moves westwards cannot be excluded, because of the mineralization of the detritus from the upper layer and mixing with deep waters (Crise et al., 1999). Moreover, the nitracline is shallower (200–750 m) in the Ionian than in the Levantine convective region (200–1000 m). In contrast, the phosphates (Fig. 17c) are higher in the Levantine (~ 0.25 mmol m^{-3}) than in the southern Ionian (<0.18 mmol m^{-3}).

The link between nitrates and phosphates has also been briefly explored by N/P molar ratios calculated from the volume-averaged concentrations in the deep layer (>1500 m). They result 27.17 for the southern Ionian, 18.36 for the northern Levantine and 14.71 for the southern Levantine basin (the averaged concentrations are listed in Table 5). From a systematic standpoint, these values are certainly in contrast to the well known N/P ratio anomaly in the Eastern Mediterranean Sea (Krom et al., 1991; Kress and Herut, 2001). It should be stressed that the primary aim of this study is the construction of climatological profiles for checking the quality of future incoming data and at the present time, the scope was not to establish whether the phosphorous is a limiting factor for the pelagic waters across the Eastern Mediterranean. In order to elucidate these discrepancies, we have simply divided our data set in two periods: (i) from the beginning of historical data up to 1985, and (ii) from 1985 onwards (i.e. from the starting of basin wide systematic observations conducted in the Eastern Mediterranean within
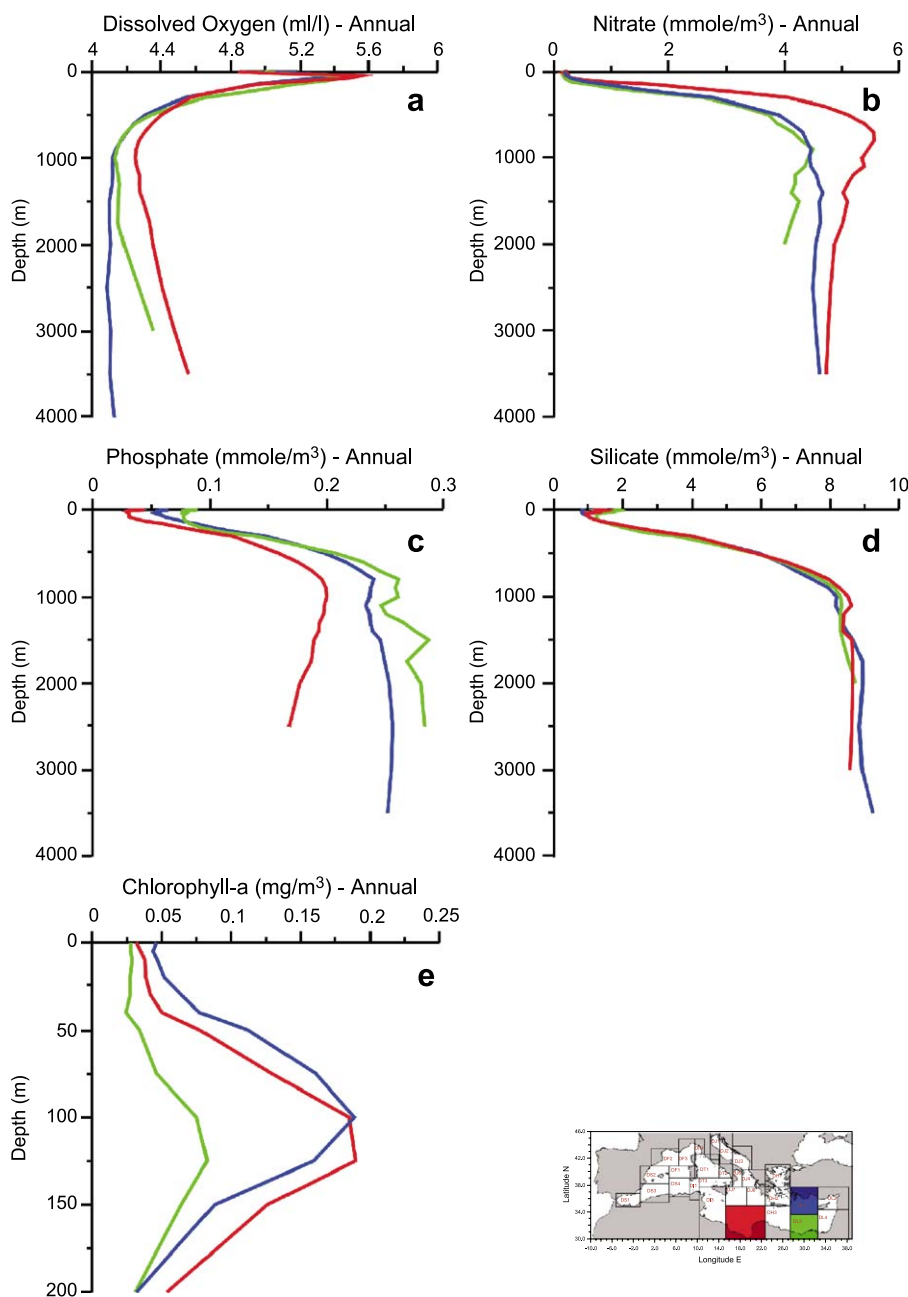
Fig. 17. Annually averaged vertical profiles of hydrographic parameters: (a) dissolved oxygen, (b) nitrate, (c) phosphate, (d) silicate, and (e) chlorophyll-*a* concentrations in three selected regions of the Eastern Mediterranean (see inset map).

the framework of the POEM programme). In the northern Levantine basin, the nitrate concentrations before 1985 result appreciably lower and phosphate higher than those obtained during the more recent

expeditions, i.e. after 1985. The reason is not known and may be due to the limited accuracies of the measurements and poor spatial coverage. On the other hand, the nitrates and phosphates in the Ionian

have resulted to be of comparable magnitude. Civitarese et al., 1998 have hypothesised that the large excess of nitrates in the Ionian Sea could be a direct consequence of the enriched dense waters of Adriatic origin that may support high molar ratios in the Eastern Mediterranean.

Comparable profiles are observed in the silicate content (Fig. 17d) that may be explained by slower decay of siliceous biogenic materials than nitrogeneous components (Yilmaz and Tuğrul, 1998). The silicate gradient zone extends down to ∼1000 m, the depth level which defines the upper boundary of the EMDW; however, the general thermohaline circulation in the deep layer does not permit to distinguish EMDW masses of different ages from silicate concentrations.

The averaged maxima of chlorophyll-*a* vary spatially and they range on an annual basis between 0.05 and 0.20 mg m^{-3}. A distinct chlorophyll-*a* maximum is observed in all regions, and it is shallower in the northern Levantine basin than in the other regions, in agreement with the major dynamical features (Yacobi et al., 1995).

5. Summary and conclusions

Seasonally averaged vertical profiles of temperature, salinity, dissolved oxygen, nutrients (nitrate, phosphate and silicate) and chlorophyll-*a* have been computed for different regions of the Mediterranean Sea, following the joint effort in rescuing, quality

Table 4

Spatially averaged water properties in four regions of the Western Mediterranean

Water mass	Temperature (°C)	Salinity (psu)	Oxygen (ml l^{-1})	Nitrate (mmol m^{-3})	Phosphate (mmol m^{-3})	Silicate (mmol m^{-3})
Gulf of Lions—DF2						
Surface water (0–5 m)	17.61±2.30 (14,218)	37.88±0.45 (9472)	5.44±0.24 (2182)	1.45±2.10 (352)	0.13±0.12 (757)	1.37±1.01 (820)
LIW (400 m)	13.17±0.11 (3101)	38.48±0.03 (2306)	4.48±0.17 (610)	6.31±0.58 (55)	0.34±0.08 (208)	6.26±1.02 (87)
WMDW (≥1500 m)	13.04±0.02 (3218)	38.42±0.01 (3473)	4.60±0.07 (1214)	7.78±0.51 (17)	0.39±0.04 (184)	8.16±0.71 (128)
Tyrrhenian North—DT1						
Surface water (0–5 m)	18.90±2.54 (11,208)	37.91±0.25 (2867)	5.55±0.26 (576)	0.24±0.22 (110)	0.08±0.07 (282)	2.17±0.59 (168)
LIW (500 m)	13.88±0.13 (593)	38.65±0.03 (391)	4.29±0.13 (179)	5.91±0.56 (32)	0.31±0.07 (61)	6.85±0.79 (29)
TDW (≥1500 m)	13.21±0.04 (277)	38.47±0.02 (185)	4.32±0.13 (139)	7.32±0.74 (10)	0.42±0.08 (20)	7.73±0.66 (12)
Algerian East—DS4						
Surface water (0–5 m)	19.56±2.52 (7684)	37.12±0.14 (1112)	5.31±0.33 (340)	0.05±0.10 (207)	0.04±0.05 (307)	0.99±0.33 (90)
LIW (500 m)	13.30±0.09 (988)	38.52±0.02 (459)	4.14±0.12 (168)	8.90±0.40 (36)	0.40±0.07 (81)	7.58±0.89 (26)
WMDW (≥1500 m)	13.04±0.04 (778)	38.42±0.02 (548)	4.49±0.12 (287)	8.28±0.11 (39)	0.39±0.05 (73)	9.29±0.27 (29)
Alboran Sea—DS1						
Surface water (0–5 m)	17.85±0.616 (18,874)	36.57±0.28 (7122)	5.44±0.33 (1877)	0.44±0.49 (733)	0.11±0.11 (1046)	1.33±1.20 (642)
LIW (500 m)	13.07±0.08 (2014)	38.45±0.04 (1588)	4.21±0.17 (320)	8.49±0.89 (126)	0.37±0.07 (121)	8.36±1.22 (112)
WMDW (≥1500 m)	13.08±0.03 (176)	38.44±0.01 (170)	4.50±0.09 (21)	9.13±3.91 (6)*	0.41±0.06 (8)*	8.381±0.99 (7)

Average and standard deviation for physical and biochemical parameters (the number of data used are indicated within brackets) for three layers, which essentially characterize the water column structure. The regions are those defined according to the scheme in Figs. 5 and 6.

  * The deepest values are at 1400 m.

checking and archiving hydrographic and biochemical data within the EU/MEDAR/MEDATLAS II and EU/MTPII/MATER data management activities. The regions are defined according to the schematic representation of the sub-basin scale dynamics, mostly representative of the upper/external thermohaline cell circulation. This method overcomes the pure definition of climatologies based on a regular grid, which, if coarsely defined, may be inadequate to resolve the complicate geometry of the Mediterranean basin. On the other hand, high-resolution gridded climatologies may result poor in statistics due to a limited number of hydrological casts in some oceanic domains.

The inhomogeneous distribution of historical data as well as coastal data can introduce biases in the seasonally averaged vertical profiles, resulting in enlarged and unrealistic variations along the vertical. For this reason, an iterative process in computing first-order statistics and annual means for the deep waters have been used, considering that some anomalous values exist in the databases. Data departing from the mean by more than one standard deviation were rejected for the computed climatologies. In addition,

data relevant to particular periods have revealed large differences with respect to the past climatologies, as for example, the large climatic shift in the temperature and salinity caused by the EMT. Analyses of measurements made since the early 1950s allowed to evidence warming trends and salinity increases in the Ionian and Levantine basin, which have resulted to be of the same order of magnitude as similar changes observed by Béthoux et al. (1990) in their pilot study in the Western Mediterranean.

A synthetic description of the dominant features in the vertical distributions of the hydrographic fields is presented on a seasonal basis from the climatological profiles in the upper waters (0–200 m). The hydrological structures along the vertical reflect the water mass distributions and their circulation patterns with satisfying accuracy. The chemical profiles follow the well-known ventilation mechanisms of the convection regions in the Gulf of Lions, in the southern Adriatic Sea and in the northern Levantine basin. In addition, several important aspects of the advective processes that transport water masses among the adjacent basins are easily identified from the transformation of water characteristics.

Table 5
As for Table 4 but in three regions of the Eastern Mediterranean

Water mass	Temperature (°C)	Salinity (psu)	Oxygen (ml l^{-1})	Nitrate (mmol m^{-3})	Phosphate (mmol m^{-3})	Silicate (mmol m^{-3})
Ionian South—DJ5						
Surface water (0–5 m)	20.26±2.49 (6208)	38.40±0.19 (545)	4.85±0.20 (531)	0.23±0.29 (103)	0.04±0.04 (244)	1.22±1.01 (139)
LIW (250 m)	14.72±0.18 (2390)	38.85±0.06 (284)	4.67±0.13 (279)	3.24±0.73 (49)	0.10±0.04 (108)	3.22±0.97 (68)
EMDW (≥1500 m)	13.70±0.02 (878)	38.69±0.02 (410)	4.40±0.11 (418)	4.89±0.37 (103)	0.18±0.04 (146)	8.65±0.49 (95)
Levantine North—DL1						
Surface water (0–5 m)	21.72±2.20 (8816)	39.16±0.10 (1995)	5.06±0.26 (1395)	0.21±0.24 (450)	0.06±0.05 (513)	0.89±0.78 (465)
LIW (125 m)	15.69±0.44 (4479)	39.02±0.05 (1087)	5.05±0.20 (720)	0.62±0.54 (237)	0.08±0.07 (313)	1.36±0.99 (262)
EMDW (≥1500 m)	13.77±0.04 (1973)	38.73±0.05 (972)	4.10±0.17 (1191)	4.59±0.92 (351)	0.25±0.07 (383)	8.94±1.47 (396)
Levantine South—DL3						
Surface water (0–5 m)	23.05±2.26 (5890)	38.97±0.39 (1116)	5.00±0.40 (1240)	0.21±0.42 (157)	0.09±0.04 (444)	1.86±1.70 (329)
LIW (125 m)	15.60±0.29 (2461)	38.97±0.06 (311)	5.03±0.15 (296)	1.13±0.63 (54)	0.09±0.05 (152)	1.92±1.23 (127)
EMDW (≥1500 m)	13.70±0.03 (632)	38.72±0.04 (309)	4.22±0.11 (385)	4.12±1.20 (90)	0.28±0.09 (129)	8.55±1.65 (96)*

* The deepest values are at 1400 m.

Table 4 summarises the layer-averaged hydrographic properties and nutrient concentrations calculated for four regions in the Western Mediterranean, i.e. the Gulf of Lions, the Tyrrhenian Sea and the Algerian basin, discussed in the text. The Alboran Sea, through which the entire Mediterranean Sea exchanges water with the Atlantic Ocean across the Strait of Gibraltar, has been also included. In Table 5, a summary of the most important water mass properties and their vertical and spatial differences in three regions of the Eastern Mediterranean, i.e. the Southern Ionian, the northern Levantine basin and the southern Levantine basin, is presented. The hydrochemical properties in the marginal basins of the Eastern Mediterranean, i.e. in the southern Adriatic Sea and in the Strait of Sicily are summarised in Table 6. The characteristics and transformations of the main water masses mentioned in the text (i.e. AW, LIW, TDW, WMDW and EMDW) can be traced from the source regions through the basin interior by a comparative analysis of the averaged values. The water column has been schematised in three layers, which essentially characterise the thermohaline circulation. The surface layer (0–5 m) may be considered representative of the AW, the properties in the LIW layer are those corresponding to the depth of the salinity maximum and finally, the properties in the deep layer (i.e. the layer essentially occupied by the TDW, WMDW and EMDW) are those calculated for depths greater than

1500 m where the waters exhibit rather homogeneous behaviour during the entire annual cycle.

The layer-averaged water mass properties and the averaged vertical profiles may be used as a basis for validating incoming data from operational oceanography and to initialise coupled physical–biological models. The full set of spatially averaged hydrological profiles can be found and downloaded from the World Wide Web data server at the OGS (http://doga.ogs.trieste.it/medar/climatologies/).

New optimisation criteria may reduce the effects of errors and uncertainties in quality control of historical data of unknown origin before incorporating them into large databases. Trend evaluations could be effective in reducing subjective choices, especially in the deep waters, when sufficiently long time-series will be available to the scientific community.

Acknowledgements

Table 6
As for Table 4 but in two marginal regions of the Eastern Mediterranean: the Southern Adriatic and the Strait of Sicily

Water mass	Temperature (°C)	Salinity (psu)	Oxygen (ml l^{-1})	Nitrate (mmol m^{-3})	Phosphate (mmol m^{-3})	Silicate (mmol m^{-3})
Adriatic South—DJ3						
Surface water (0–5 m)	16.58±2.53 (14,218)	37.93±0.69 (9739)	5.47±0.26 (3000)	0.57±0.47 (1665)	0.04±0.03 (2442)	2.86±1.43 (1201)
LIW (200 m)	13.63±0.18 (1351)	38.70±0.04 (1039)	4.97±0.22 (372)	4.98±0.70 (235)	0.18±0.05 (244)	5.38±1.32 (210)
ADW (≥1000 m)	12.88±0.05 (812)	38.59±0.01 (768)	4.89±0.18 (272)	5.25±0.65 (208)	0.19±0.05 (245)	9.67±2.61 (193)
Sicily Strait—DI3						
Surface water (0–5 m)	19.23±2.59 (11,709)	37.47±0.20 (3476)	5.25±0.37 (1468)	0.48±0.76 (455)	0.06±0.06 (526)	1.09±0.59 (189)
LIW (400 m)	14.02±0.13 (1823)	38.75±0.02 (678)	4.30±0.13 (215)	5.46±0.87 (54)	0.20±0.05 (64)	7.25±1.33 (47)
EMDW (≥1500 m)	13.83±0.04 (12)	38.73±0.01 (10)	4.21±0.01 (4)	5.00±0.31 (2)*	0.18±0.04 (4)*	5.89±1.29 (4)**

* The deepest value is at 1200 m.
** The deepest value is at 1000 m.

References

Artegiani, A., Bregant, D., Paschini, E., Pinardi, N., Raicich, F., Russo, A., 1997. The Adriatic Sea general circulation: Part I. Air–sea interaction and water mass structure: Part II. Baroclinic circulation structure. J. Phys. Oceanogr. 27, 1492–1532.

Astraldi, M., Gasparini, G.P., Vetrano, A., Vignudelli, S., 2002. Hydrographic characteristics and interannual variability of water masses in the central Mediterranean: a sensitivity test for long-term changes in the Mediterranean Sea. Deep-Sea Res., Part 1, Oceanogr. Res. Pap. 49, 661–680.

Béthoux, J.P., Gentili, B., Raunet, J., Taillez, D., 1990. Warming trend in the Western Mediterranean deep water. Nature 347, 660–662.

Béthoux, J.P., Morin, P., Madec, C., Gentili, B., 1992. Phosphorus and nitrogen behaviour in Mediterranean Sea. Deep-Sea Res. 39, 1641–1654.

Bignami, F., Salusti, E., Schiarini, S., 1990. Observations on a bottom vein of dense water in the Southern Adriatic and Ionian Seas. J. Geophys. Res. 95, 7249–7259.

Castellari, S., Pinardi, N., Leaman, K., 2000. Simulation of water mass formation processes in the Mediterranean Sea: influence of the time frequency of atmospheric forcing. J. Geophys. Res. 105, 24157–24181.

CIESM, 2002. Tracking long-term hydrological change in the Mediterranean Sea. In: Briand, F. (Ed.), 2002. CIESM Workshop Series, vol. 16, p. 134.

Civitarese, G., Gacic, M., Vetrano, A., Boldrin, A., Bregant, D., Rabitti, S., Souvermezoglou, E., 1998. Biochemical fluxes through the Strait of Otranto (Eastern Mediterranean). Cont. Shelf Res. 18, 773–789.

Coatanoan, C., Metzl, N., Fieux, M., Coste, B., 1999. Seasonal water mass distribution in the Indonesian throughflow entering the Indian Ocean. J. Geophys. Res. 104, 20801–20826.

Coste, B., Gostan, J., Minas, H.J., 1972. Influence des conditions hivernales sur les productions phyto-et zooplanctoniques en Méditerranée Nord-Occidentale: I. Structures hydrologiques et distribution des sels nutritifs. Mar. Biol. 16, 320–348.

Crise, A., Allen, J.I., Baretta, J., Crispi, G., Mosetti, R., Solidoro, C., 1999. The Mediterranean pelagic ecosystem response to physical forcing. Prog. Oceanogr. 44, 219–243.

Denis-Karafistan, A., Martin, J.M., Minas, H., Brasseur, P., Nihoul, J., Denis, C., 1998. Space and seasonal distributions of nitrates in the Mediterranean Sea derived from a variational inverse model. Deep-Sea Res., Part 1, Oceanogr. Res. Pap. 45, 387–408.

Gacic, M., Civitarese, G., Miserocchi, S., Cardin, V., Crise, A., Mauri, E., 2002. The open-ocean convection in the Southern Adriatic: a controlling mechanism of the spring phytoplankton bloom. Cont. Shelf Res. 22, 1897–1908.

Guibout, P., 1987. Atlas Hydrographique de la Mediterranée IFRMER, Brest.

Hopkins, T.S., 1978. Physical Processes in the Mediterranean basins. In: Kjerfve, B. (Ed.), Estuarine Transport Processes. Univ. of South Carolina Press, Columbia, SC, pp. 269–310.

Kinder, T.H., Parilla, G., 1987. Yes, some of the Mediterranean outflow does come from great depth. J. Geophys. Res. 92, 2901–2906.

Klein, B., Roether, W., Manca, B., Bregant, D., Beitzel, V., Kovacevic, V., Luchetta, A., 1999. The large deep transient in the Eastern Mediterranean. Deep-Sea Res., Part 1, Oceanogr. Res. Pap. 46, 371–414.

Kress, N., Herut, B., 2001. Spatial and seasonal evolution of dissolved oxygen and nutrients in the Southern Levantine basin (Eastern Mediterranean Sea): chemical characterization of the water masses and inferences on the N:P ratios. Deep-Sea Res., Part 1, Oceanogr. Res. Pap. 48, 2347–2372.

Krom, M.D., Kress, N., Brenner, S., Gordon, L.I., 1991. Phosphorus limitation of primary productivity in the E. Mediterranean sea. Limnol. Oceanogr. 36, 424–432.

Krom, M.D., Brenner, S., Kress, N., Neori, A., Gordon, L.I., 1992. Nutrient dynamics and new production in a warm-core eddy from the Eastern Mediterranean Sea. Deep-Sea Res. 39, 467–480.

Lascaratos, A., Roether, W., Nittis, K., Klein, B., 1999. Recent changes in deep water formation and spreading in the Eastern Mediterranean Sea. Prog. Oceanogr. 44, 5–36.

Leaman, K.D., Schott, F.A., 1991. Hydrographic structure of the convective regime in the Gulf of Lions: Winter 1987. J. Phys. Oceanogr. 21, 573–596.

Levitus, S., 1982. Climatological atlas of the world ocean. NOAA Professional Paper, vol. 13. U.S. Gov. Printing Office, Washington, DC. 173 pp.

Levitus, S., Boyer, T., Conkright, M., O'Brien, T., Antonov, J., Stephens, C., Stathoplos, L., Johnson, D., Gelfed, R., 1998. World Ocean Database 1998, vol. 1: Introduction. NOAA Atlas NESDIS 18, Washington, DC. 346 pp.

Lipiatou, E., Heussner, S., Mosetti, R., Tintoré, J., Tselepides, A. (Eds.), 1999. Progress in oceanography of the Mediterranean Sea. Spec. Issue, Prog. Oceanogr., vol. 44, p. 468.

Maillard, C., Fichaut, M., MEDAR/MEDATLAS Group, 2001. MEDAR-MEDATLAS Protocol (V3) Part I: Exchange Format and Quality Checks for Observed Profiles; Rap. Int. IFREMER, Brest. TMSI/IDM/SISMER/SIS00-084.

Maillard, C., Balopoulos, E., Giorgetti, A., Fichaut, M., Iona, A., Larour, M., Latrouite, A., Manca, B., Maudire, G., Nicolas, P., Sanchez-Cabeza, J.-A., 2002. An integrated system for managing multidisciplinary oceanographic data collected in the Mediterranean Sea during the basin-scale research project EU/MAST-MATER (1996–2000). J. Mar. Syst. 33–34, 523–538.

Malanotte-Rizzoli, P., 1991. The Northern Adriatic Sea as a prototype of convection and water mass formation on the continental shelf. In: Chu, P.C., Gascard, J.C. (Eds.), Deep Convection and Deep Water Formation in the Oceans. Elsevier Oceanography Series, vol. 57. Elsevier, Amsterdam, pp. 229–239.

Malonotte-Rizzoli, P., Manca, B.B., Ribera d'Alcalà, M., Theocharis, A., Bergamasco, A., Bregant, D., Budillon, G., Civitarese, G., Georgopoulos, D., Michelato, A., Sansone, E., Scarazzato, P., Souvermezoglou, E., 1997. A synthesis of the Ionian Sea hydrography, circulation and water mass pathways during POEM-Phase I. Prog. Oceanogr. 39, 153–204.

Malanotte-Rizzoli, P., Manca, B.B., Ribera d'Alcalà, M., Theocharis, A., Brenner, S., Budillon, G., Özsoy, E., 1999. The Eastern Mediterranean in the 80s and in the 90s: the big transition in the intermediate and deep circulations. Dyn. Atmos. Ocean. 29, 365–395.

Manca, B., Giorgetti, A., 1998. Thermohaline properties and circulation patterns in the Southern Adriatic Sea from May 1995 to February 1996. In: Piccazzo, M. (Ed.), Atti del 12° Congresso dell'Associazione Italiana di Oceanografia e Limnologia (Isola di Vulcano, 18–21 Settembre 1996), vol. II. A.I.O.L, Genova, 399–414.

Manca, B.B., Kovacevic, V., Gacic, M., Viezzoli, D., 2002. Dense water formation in the Southern Adriatic sea and spreading into the Ionian Sea in the period 1997–1999. J. Mar. Syst. 33–34, 133–154.

Martin, J.-M., Milliman, J.D., 1997. EROS 2000 (European River Ocean System). The western Mediterranean: an introduction. Deep-Sea Res., Part 2, Top. Stud. Oceanogr. 44, 521–529.

Marullo, S., Santoleri, R., Malanotte-Rizzoli, P., Bergamasco, A., 1999. The sea surface temperature field in the Eastern Mediterranean from AVHRR data: Part I. Seasonal variability: Part II. Interannual variability. J. Mar. Syst. 20, 63–112.

MEDAR Group, 2002. MEDATLAS 2002 Mediterranean and Black Sea database of temperature, salinity and biochemical parameters climatological atlas, 4 CD-ROM. European Commission Marine Science and Technology Programme (MAST). Ed. IFREMER (sismer@ifremer.fr), Brest.

MEDATLAS Consortium, 1997. Mediterranean Hydrological Atlas of temperature and salinity. A MAST support initiative for ocean data and information management, Contr. No. MAS2-CT93-0074, Coordinating Center IFREMER/SISMER Centre de Brest, France (C. Maillard), three CD-ROM, IFREMER Ed.

MEDOC Group, 1970. Observation of formation of deep water in the Mediterranean Sea. Nature 277, 1037–1040.

Miller, A.R., Tchernia, P., Charnock, H., Mc Gill, D.A., 1970. Mediterranean Sea Atlas of temperature, salinity, oxygen profiles and data from cruises of R.V. Atlantis and R/V chain with distribution of nutrient chemical properties. Woods Hole Oceanographic Institution Atlas Series, vol. 3. Woods Hole Oceanographic Instit., Woods Hole, MA.

Millot, C., 1991. Mesoscale and seasonal variabilities of the circulation in the western Mediterranean. Dyn. Atmos. Ocean. 15, 179–214.

Millot, C., 1995. PRIMO-0 and related experiments. Oceanol. Acta 18, 137–138.

Millot, C., 1999. Review paper circulation in the Western Mediterranean Sea. J. Mar. Syst. 20, 423–442.

MODB Group (The), 1996. Climatological Atlas of the Mediterranean Sea. Scientific Report of the MAST-MODB initiative for ocean data and information management, Contr. No. MAS2.0093.0075. BE, University of Liège, Liège.

Monaco, A., Peruzzi, S., 2002. The Mediterranean targeted project MATER—a multiscale approach of the variability of a marine system—overview. J. Mar. Syst. 33–34, 3–21.

Mosetti, F., 1983. Fundamental features of the Adriatic Sea hydrology. In: Universita' degli studi di Trieste (Ed.), Atti del convegno internazionale 'I problemi del mare Adriatico', Trieste, 26–27 Settembre 1983. Università degli studi di Trieste, Trieste, pp. 209–239.

Napolitano, E., Oguz, T., Malanotte-Rizzoli, P., Yilmaz, A., Sansone, E., 2000. Simulations of biological production in the Rhodes and Ionian basins of the eastern Mediterranean. J. Mar. Syst. 24, 277–298.

Ovchinnikov, I.M., Zats, V.I., Krvosheya, V.G., Udodov, A.I., 1985. Formation of Deep Eastern Mediterranean waters in the Adriatic Sea. Oceanology 25 (6), 704–707.

Özsoy, E., Latif, M.A., 1996. Climate variability in the Eastern Mediterranean and the great Aegean outflow anomaly. In: Denis, M. (Ed.), (Ed.), POEM-BC Workshop, Molitg les Bains, France, 1–5 July 1996. Centre d'Océanologie de Marseille, Marseille, pp. 69–86.

Özsoy, E., Hecht, A., Unluata, U., Brenner, S., Sur, H.I., Bishop, J., Latif, M.A., Rozentraub, Z., Oguz, T., 1993. A synthesis of the Levantine Basin circulation and hydrography, 1985–1990. Deep-Sea Res., Part 2, Top. Stud. Oceanogr. 40, 1075–1119.

Picco, P., 1990. Climatological Atlas of the Western Mediterranean. ENEA, Roma. 224 pp.

Pinardi, N., Korres, G., Lascaratos, A., Roussenov, V., Stanev, E., 1997. Numerical simulation of the interannual variability of the Mediterranean Sea upper ocean circulation. Geophys. Res. Lett. 24, 425–428.

POEM Group (The), 1992. General circulation of the Eastern Mediterranean Sea. Earth-Sci. Rev. 32, 285–308.

Prieur, L., Sournia, A., 1994. 'Almofront-1' (April–May 1991): an interdisciplinary study of the Almaria-Oran geostrophic front, SW Mediterranean Sea. J. Mar. Syst. 3–5, 187–203.

Reid, J.L., 1979. On the contribution of the Mediterranean Sea outflow to the Norwegian–Greenland Sea. Deep-Sea Res. 26A, 1199.

Reiniger, R.F., Ross, C.K., 1968. A method of interpolation with application to oceanographic data. Deep-Sea Res. 15, 185–193.

Robinson, A.R., Malanotte-Rizzoli, P. (Eds.), 1993. Physical Oceanography of the Eastern Mediterranean. Deep-Sea Res., Part 2, Top. Stud. Oceanogr., vol. 40, pp. 1073–1332.

Robinson, A.R., Golnaraghi, M., Leslie, W.G., Artegiani, A., Hecht, A., Lazzoni, E., Michelato, A., Sansone, E., Theocharis, A., Ünlüata, Ü., 1991. The eastern Mediterranean general circulation: features, structure and variability. Dyn. Atmos. Ocean. 15, 215–240.

Robinson, A.R., Leslie, W., Theocharis, A., Lascaratos, A., 2001. Mediterranean Sea circulation. Encyclopedia of Ocean Science, vol. 3. Academic Press, San Diego, CA, pp. 1689–1705.

Roether, W., Well, R., 2001. Oxygen consumption in the Eastern Mediterranean. Deep-Sea Res., Part 1, Oceanogr. Res. Pap. 48, 1535–1551.

Roether, W., Manca, B., Klein, B., Bregant, D., Georgopoulos, D.,

Artegiani, A., Kovacevic, V., Luchetta, A., 1996. Recent changes in Eastern Mediterranean deep waters. Science 271, 333–335.

Roether, W., Klein, B., Beitzel, V., Manca, B.B., 1998. Property distributions and transient-tracer ages in Levantine Intermediate Water in the Eastern Mediterranean. J. Mar. Syst. 18, 71–87.

Rohling, E.J., Bryden, H.L., 1992. Man-induced salinity and temperature increase in the western Mediterranean deep water. J. Geophys. Res. 97, 11191–11198.

Roussenov, V., Stanev, E., Artale, V., Pinardi, N., 1995. A seasonal model of the Mediterranean Sea general circulation. J. Geophys. Res. 100, 13515–13538.

Schlitzer, R., Roether, W., Oster, H., Junghans, H.-G., Hausmann, M., Johannsen, H., Michelato, A., 1991. Chlorofluoromethane and oxygen in the Eastern Mediterranean. Deep-Sea Res. 38, 1531–1551.

Sparnocchia, S., Manzella, G.M., La Violette, P., 1994. The interannual and seasonal variability of the MAW and LIW core properties in the Western Mediterranean. In: La Violette, P.E. (Ed.), The Seasonal and Interannual Variability of the Western Mediterranean Sea. Coastal and Estuarine Studies, vol. 46. AGU, Augsburg, pp. 177–194.

Sparnocchia, S., Gasparini, G.P., Astraldi, M., Borghini, M., Pistek, P., 1999. Dynamics and mixing of the Eastern Mediterranean outflow in the Tyrrhenian basin. J. Mar. Syst. 20, 301–317.

Sur, H.I., Özsoy, E., Ünlüata, Ü., 1992. Simultaneous deep and intermediate depth convection in the northern Levantine Sea, winter 1992. Oceanol. Acta 16, 33–43.

Theocharis, A., Lascaratos, A., Sofianos, S., 2002. Variability of sea water properties in the Ionian, Cretan and Levantine seas during the last century. In: Briand, F. (Ed.), Tracking long-term hydrological change in the Mediterranean Sea. CIESM Workshop Series, vol. 16, pp. 73–76.

UNESCO, 1993. CEC/DG XII, MAST and IOC/IODE, Manual of Quality Control Procedures for Validation of Oceanographic Data. IOC Manual and Guides, vol. 26, p. 436.

Wu, P., Haines, K., 1998. The general circulation of the Mediterranean Sea from 100-year simulation. J. Geophys. Res. 103, 1121–1135.

Yacobi, Y.Z., Zohary, T., Kress, N., Hecht, A., Robarts, R.D., Waiser, M., Wood, A.M., Li, W.K.W., 1995. Chlorophyll distribution throughout the southeastern Mediterranean in relation to the physical structure of the water mass. J. Mar. Syst. 6, 179–190.

Yilmaz, A., Tuğrul, S., 1998. The effect of cold- and warm-core eddies on the distribution and stoichiometry of dissolved nutrients in the northeastern Mediterranean. J. Mar. Syst. 16, 253–268.

Zavatarelli, M., Raicich, F., Bregant, D., Russo, A., Artegiani, A., 1998. Climatological biochemical characteristics of the Adriatic Sea. J. Mar. Syst. 18, 227–263.